AD-A045 181 ARMY MISSILE RESEARCH AND DEVELOPMENT COMMAND REDSTO--ETC F/G 4/2
INFRARED AND SUBMILLIMETER EXTINCTION BY FOG.(U)
JUL 77 D A STEWART
UNCLASSIFIED DRDMI-TR-77-9 NL

1 OF 1
AD
A045181

END
DATE
FILMED
11-77
DDC

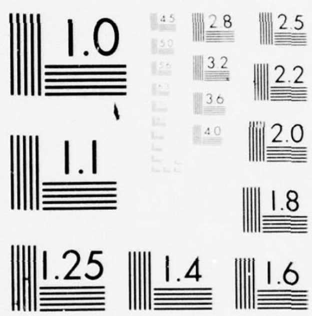

MICROCOPY RESOLUTION TEST CHART
NATIONAL BUREAU OF STANDARDS-1963-A

AD A 045181

U.S. ARMY MISSILE RESEARCH AND DEVELOPMENT COMMAND

TECHNICAL REPORT TR-77-9

INFRARED AND SUBMILLIMETER EXTINCTION BY FOG

Physical Sciences Directorate
Technology Laboratory

14 July 1977

Approved for public release; distribution unlimited.

Redstone Arsenal, Alabama 35809

DMI FORM 1000, 1 APR 77

DISPOSITION INSTRUCTIONS

DESTROY THIS REPORT WHEN IT IS NO LONGER NEEDED. DO NOT RETURN IT TO THE ORIGINATOR.

DISCLAIMER

THE FINDINGS IN THIS REPORT ARE NOT TO BE CONSTRUED AS AN OFFICIAL DEPARTMENT OF THE ARMY POSITION UNLESS SO DESIGNATED BY OTHER AUTHORIZED DOCUMENTS.

TRADE NAMES

USE OF TRADE NAMES OR MANUFACTURERS IN THIS REPORT DOES NOT CONSTITUTE AN OFFICIAL INDORSEMENT OR APPROVAL OF THE USE OF SUCH COMMERCIAL HARDWARE OR SOFTWARE.

UNCLASSIFIED

SECURITY CLASSIFICATION OF THIS PAGE (When Data Entered)

REPORT DOCUMENTATION PAGE

READ INSTRUCTIONS BEFORE COMPLETING FORM

1. REPORT NUMBER

14 DRDMI-TR-77-9

2. GOVT ACCESSION NO.

3. RECIPIENT'S CATALOG NUMBER

4. TITLE (and Subtitle)

6 INFRARED AND SUBMILLIMETER EXTINCTION BY FOG.

5. TYPE OF REPORT & PERIOD COVERED

9 Technical Report

6. PERFORMING ORG. REPORT NUMBER

TR-77-9

7. AUTHOR(s)

10 Dorathy Anne Stewart

8. CONTRACT OR GRANT NUMBER(s)

16

9. PERFORMING ORGANIZATION NAME AND ADDRESS

Commander
US Army Missile Research and Development Command
Attn: DRDMI-TR
Redstone Arsenal, Alabama 35809

10. PROGRAM ELEMENT, PROJECT, TASK AREA & WORK UNIT NUMBERS

DA 1L161102AH49 17 00
AMCMS Code 611102.H490011

11. CONTROLLING OFFICE NAME AND ADDRESS

11 Commander
US Army Missile Research and Development Command
Attn: DRDMI-TI
Redstone Arsenal, Alabama 35809

12. REPORT DATE

14 July 1977

13. NUMBER OF PAGES

~~61~~ 12 49p.

14. MONITORING AGENCY NAME & ADDRESS (if different from Controlling Office)

15. SECURITY CLASS. (of this report)

UNCLASSIFIED

15a. DECLASSIFICATION/DOWNGRADING SCHEDULE

16. DISTRIBUTION STATEMENT (of this Report)

Approved for public release; distribution unlimited.

17. DISTRIBUTION STATEMENT (of the abstract entered in Block 20, if different from Report)

18. SUPPLEMENTARY NOTES

19. KEY WORDS (Continue on reverse side if necessary and identify by block number)

Fog drop sizes
Visibility
Infrared
Submillimeter
Propagation

20. ABSTRACT (Continue on reverse side if necessary and identify by block number)

A thorough literature survey of fog drop-size distributions throughout the world is discussed, and data from 36 references are summarized.

The review of an extensive list of over 100 references includes additional important information. Ranges of liquid water content and problems of relating this to over

ABSTRACT (Continued)

DD FORM 1 JAN 73 1473 EDITION OF 1 NOV 65 IS OBSOLETE

UNCLASSIFIED

SECURITY CLASSIFICATION OF THIS PAGE (When Data Entered)

416211

ABSTRACT (Concluded)

visibility are examined. Changes in fog characteristics from place to place and from time to time are also considered, and the discussion includes small-scale spatial and temporal fluctuations.

A representative sample of data is used to compute extinction of electromagnetic energy with wavelengths of 0.55, 10.5, 870, and 1250 μm. Extinction of the 1250-μm wavelength by fog droplets is always less than extinction of the 870-μm wavelength. Extinction of the 870-μm energy by fog droplets is always less than extinction of the visible and the 10.5-μm energy. The relationship between the visible and the infrared extinction depends upon the drop-size distribution. The 10.5-μm wavelength is frequently attenuated about the same amount as the visible, and it is not uncommon for the infrared extinction to be greater than the visible extinction.

CONTENTS

ACKNOWLEDGMENTS

The author would like to express her appreciation to Dr. Oskar M. Essenwanger for encouragement and helpful suggestions during this project. She would also like to thank Dr. Bobby D. Guenther for calling her attention to an important publication. Personnel at Redstone Scientific Information Center deserve credit for their extra efforts to obtain some obscure publications. Finally, thanks are due to Mrs. Clara B. Brooks for her care in typing the manuscript.

I. INTRODUCTION

Fog, mist, and haze are obstructions to visibility. Fog exists when the atmosphere contains a suspended aggregate of very small water drops which reduce the horizontal visibility to 1 km or less near the surface. When an aggregate of water droplets suspended in the atmosphere near the surface does not reduce visibility as low as 1 km, it is called mist. Mist is intermediate between fog and haze. Haze consists of particles which are so small they cannot be felt or individually seen with the eye. Haze particles may be dry or damp. More detailed definitions may be found in the Glossary of Meteorology (Huschke, 1959). Eldridge (1969) discusses alternate definitions which exist in the literature.

This report is primarily concerned with fog, but first, a few references will be listed for the reader who is interested in visibilities greater than 1 km. Wells et al. (1977), Hänel (1971), Mészaros (1971), and Laktionov (1967a) contain information about the size of particles and visibility as a function of relative humidity. Johnson (1976) shows that ultragiant aerosols with radii of 15 μm and larger are not rare. Flanigan and DeLong (1970) and Hoidale and Blanco (1969) discuss measurements of infrared characteristics of dust. Gordin and Strelkov (1975) and Carlon (1970) consider infrared characteristics of very fine water aerosol.

Fog is formed by a variety of meteorological processes.

When the ground loses heat at night by radiational cooling through a clear atmosphere, radiation fog will form if the air cools enough to become supersaturated.

Advection fog is fog which forms when warm, moist air moves across water or land which has a lower temperature.

Frontal fog is associated with a frontal passage. Frontal fog may be caused by rain falling into cooler air or by mixing of different air masses near the frontal zone. Some authors call the former an evaporation fog and the latter a mixing fog.

An upslope fog is formed when air flows upward over rising terrain and cools adiabatically to the dew point.

Steam fog, which is also called evaporation fog, is formed when cold air moves over a warmer body of water or when warm rain falls through a layer of colder air.

Further information of a general nature may be found in standard references such as Berry et al. (1945), Huschke (1959), Landsberg (1958), and Schönwiese (1970).

Mathematical and numerical models describing different characteristics of fog are found in Baronti and Elzweig (1973), Lala et al. (1975), Low (1975b), Magono et al. (1974), Rodhe (1962, 1966), and Weinstein (1974a, b).

II. COMPUTATIONAL PROCEDURE

When electromagnetic energy propagates through an atmosphere which contains scattering and absorbing particles, the extinction coefficient σ, which is also called the attenuation coefficient, is given by the following formula:

$$\sigma = \sum_i \pi r_i^2 (Q_{ext})_i N_i \quad ,$$

where r_i is the radius of particles in the ith interval which contains N_i particles per cubic unit of length. To be precise, the r_i^2 which is used in the computation should be the mean square radius over the interval. $(Q_{ext})_i$ is the mean extinction efficiency factor (also called the relative extinction coefficient or the normalized extinction cross section) in the ith radius interval. Q_{ext} is a dimensionless function of drop size, wavelength of electromagnetic energy, and the complex index of refraction. The extinction coefficient σ is in units of inverse length. If σ is in units of m^{-1}, the attenuation in decibels/kilometer may be obtained by multiplying by 4343.

Johnson (1954) has shown that if one assumes a threshold of brightness contrast of 0.02, one may compute the visibility V according to the formula

$$V = \frac{3.912}{\sigma} \quad ,$$

where σ is computed for some wavelength near the middle of the visible range. If the units of σ are m^{-1}, the visibility is in meters.

Mie (1908) developed a theory to describe scattering and absorption of electromagnetic energy by spherical particles with a known complex index of refraction $m = n - ik$. Modern discussions and explanations of electromagnetic propagation theory can be found in Kerker (1969), McCartney (1976), Deirmendjian et al. (1961), Weeks (1964), Stephens et al. (1971), and Verner (1976). A summary of the procedure used in this report follows.

The extinction efficiency factor is related to the complex numbers a_n and b_n by the formula

$$Q_{ext} = \frac{2}{\alpha^2} \sum_{n=1}^{\infty} (2n + 1) [\mathrm{Re}(a_n + b_n)] \quad .$$

The dimensionless parameter α is the ratio of the circumference of the drop to the wavelength of radiant energy and is defined by

$$\alpha = \frac{2\pi r}{\lambda} \quad .$$

The wavelength λ must be expressed in the same units as the radius.

The quantities a_n and b_n are defined by

$$a_n = \frac{\psi_n(\alpha)\psi'_n(\beta) - m\psi_n(\beta)\psi'_n(\alpha)}{\zeta_n(\alpha)\psi'_n(\beta) - m\psi_n(\beta)\zeta'_n(\alpha)}$$

and

$$b_n = \frac{m\psi_n(\alpha)\psi_n'(\beta) - \psi_n(\beta)\psi_n'(\alpha)}{m\zeta_n(\alpha)\psi_n'(\beta) - \psi_n(\beta)\zeta_n'(\alpha)} \quad ,$$

where $\beta = m\alpha$ and $\zeta = \psi + i\chi$. The prime denotes differentiation with respect to the argument. The quantities ψ and χ are Ricatti-Bessel functions defined as

$$\psi_n(x) = \left(\frac{\pi x}{2}\right)^{1/2} J_{n+1/2}(x)$$

and

$$\chi_n(x) = -\left(\frac{\pi x}{2}\right)^{1/2} N_{n+1/2}(x) \quad ,$$

where $J_{n+1/2}(x)$ and $N_{n+1/2}(x)$ are half integral order Bessel and Neumann functions of any argument x.

For computational purposes, one may define the appropriate quantities for n = 0 and n = 1 and use an iterative procedure to obtain higher order terms

$$\psi_0(x) = \sin x$$

$$\psi_1(x) = \frac{\sin x}{x} - \cos x$$

$$\chi_0(x) = \cos x$$

$$\chi_1(x) = \frac{\cos x}{x} + \sin x \quad .$$

When x is a complex number such as β, the preceding functions transform into functions of hyperbolic sines and cosines according standard equations.

The equations for finding higher order terms of ψ and χ are

$$Z_{n+1}(x) = \frac{2n+1}{x} Z_n(x) - Z_{n-1}(x)$$

and

$$Z'_n(x) = \frac{n+1}{x} Z_n(x) - Z_{n+1}(x)$$

$$= \frac{1}{2n+1} \left[(n+1) Z_{n-1}(x) - n Z_{n+1}(x) \right] \quad ,$$

where Z is either ψ or χ and x is α or β.

The accuracy of the computer programs has been checked by making test calculations for comparison with tables published by the US Bureau of Standards (1949), Gumprecht and Sliepcevich (1951), Penndorf (1957), Irvine and Pollack (1968), and Appendix J of McCartney (1976). Gumprecht and Sliepcevich, Penndorf, and McCartney only deal with real indices of refraction. Irvine and Pollack's tables are quite extensive. They cover many wavelengths and a few drop radii for complex indices of refraction of water and ice. The publication by the US Bureau of Standards is particularly useful for checking computations because it includes values of a_n and b_n and it considers real and complex indices of refraction.

One might also note that Chýlek (1975, 1977) has shown that the extinction efficiency factor approaches a limiting value of two as α becomes infinite for all values of the index of refraction, but the limiting value of the scattering efficiency factor is a function of the refractive index.

Mie theory is quite reliable for spherical scatterers. For example, Dobbins and Eklund (1977) have recently shown that the smallest scale of fluctuations predicted by the theory can be measured in the laboratory.

Fog water droplets are nearly spherical, but ice particles are not spherical. Any reader interested in nonspherical particles is advised to consult Zerull et al. (1977).

Table 1 contains the indices of refraction which were used to make the computations discussed in Section IV of this report. These computations are not highly sensitive to small changes in the index of refraction, and the results would have been qualitatively the same if sources other than Davies et al. (1970) and Hale and Querry (1973) had been used.

A few other sources of data will be noted for the interested reader. Deirmendjian (1975), Downing and Williams (1975), Rozenberg (1974), Irvine and Pollack (1968), and Kislovskii (1959) contain indices of refraction for several wavelengths. Additional information about indices of refraction of water near 1 mm can be found in Chamberlain et al. (1973), Apletalin et al. (1970), and Goronina et al. (1966). The preceding references are concerned with pure water or ice, but Querry et al. (1977) have studied relative reflectance and complex refractive index in the infrared for various samples of saline environmental waters.

Figure 1 is a conventional graph of Q_{ext} versus α for wavelengths of 0.55 and 10.5 μm. This graph has been slightly smoothed because the smaller scale ripple structure is not important for our purposes.

TABLE 1. INDICES OF REFRACTION

Source	Wavelength (μm)	Index of Refraction
Hale and Querry (1973)	0.55	$1.333 - 1.96\ (10^{-9})\ i$
Hale and Querry (1973)	10.5	$1.185 - 0.0662\ i$
Davies et al. (1970)*	870	$2.422 - 0.9667\ i$
Davies et al. (1970)	1250	$2.630 - 1.1407\ i$

*The index of refraction for 870 μm is an interpolated value.

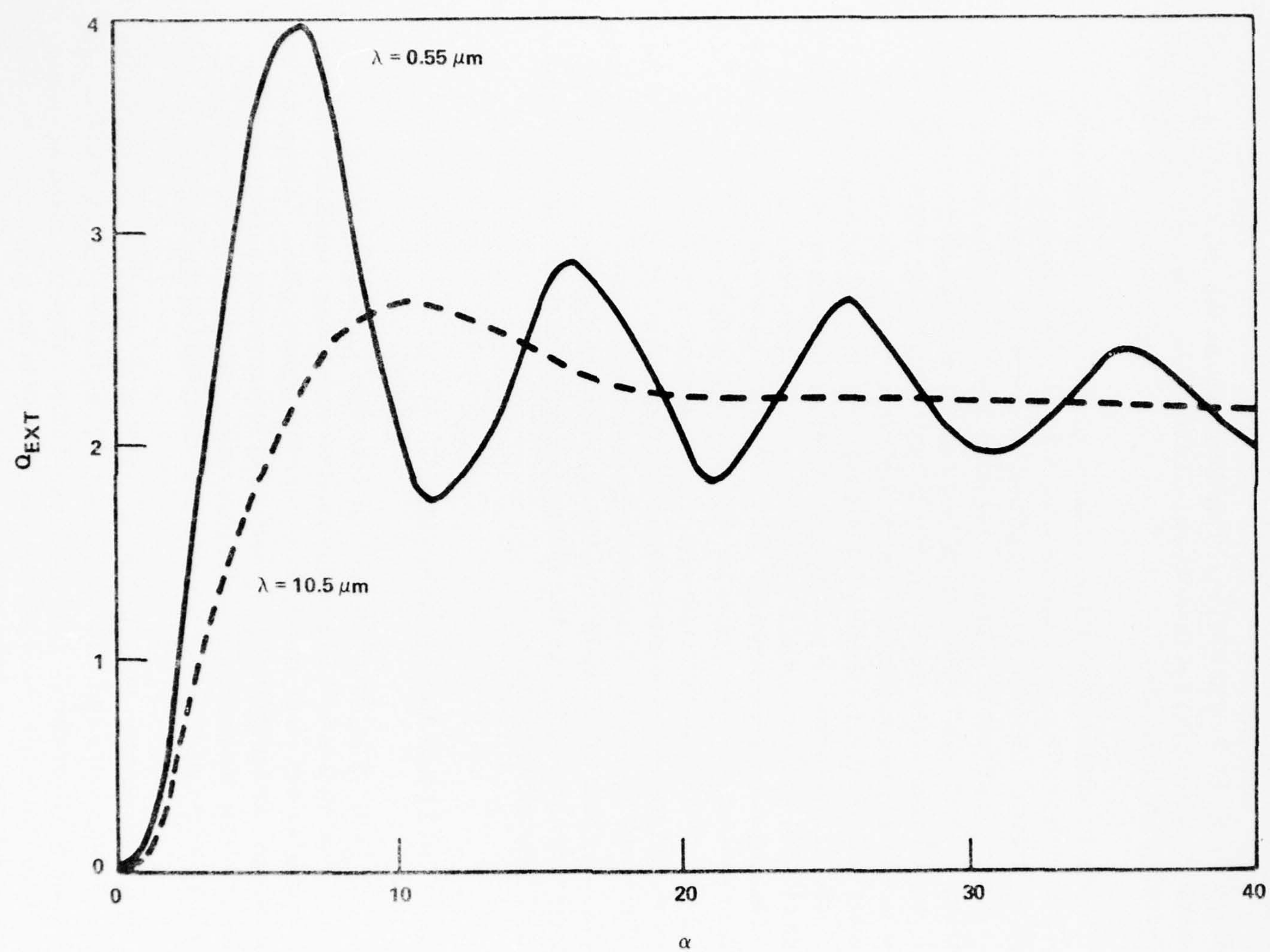

Figure 1. Q_{ext} versus α for 0.55 and 10.5 μm.

In Figure 2, Q_{ext} is graphed as a function of droplet radius for wavelengths of 0.55, 10.5, and 870 μm. This graph shows that extinction is actually greater for 10.5-μm energy than for the visible energy when particles are larger than about 10 μm in radius.

Table 2 contains a sample computation of extinction for a hypothetical fog drop-size distribution. The purpose of showing this computation is to demonstrate the relative importance of small and large drops to atmospheric extinction. It has sometimes been argued that many measurement techniques discriminate against small drops, and this computation should demonstrate the small importance of this fact. The hypothetical distribution differs from one of the measured distributions only in the first three radius intervals. No particles in the corresponding real distribution were recorded with radii less than 1 μm. There were 5.5 particles per cubic centimeter in the 1- to 2-μm radius interval and 4.8 particles per cubic centimeter in the 2- to 3-μm interval. Thus, the computed visibility for the hypothetical distribution in Table 2 is 221 m as compared with 248 m for the measured distribution. However, if the 0.9 particles per cubic centimeter with radii greater than 15 μm were removed from Table 2, and everything else remained the same, the computed visibility would be 245 m. Therefore, one sees that eliminating 170 particles per cubic centimeter with radii less than 3 μm for the distribution in Table 2 has almost the same effect as eliminating 0.9 particles per cubic centimeter with radii greater than 15 μm.

III. FOG DROP-SIZE DISTRIBUTIONS

Radii of fog drops range from less than 1 μm to slightly over 100 μm. This section will include information concerning variations from one place to another and from one fog to another in the same place. Although some variations are caused by biases in methods of measurement as suggested by Eldridge (1971), instrumental limitations cannot explain all of the variations in Table 3, which summarizes the data to be discussed in this section.

The very thorough investigation by Arnulf et al. (1957) in France is often quoted. The experimental work was done at St. Inglevert (Pas-de-Calais) near the sea and at Villacoublay, an airport near Paris. They measured drop-size distributions and extinction of several wavelengths in hazes and fogs. No radii greater than 15 μm were shown on their graphs, and the main mode was near 2.5 μm for all data. Large secondary modes did not appear. In hazes, the

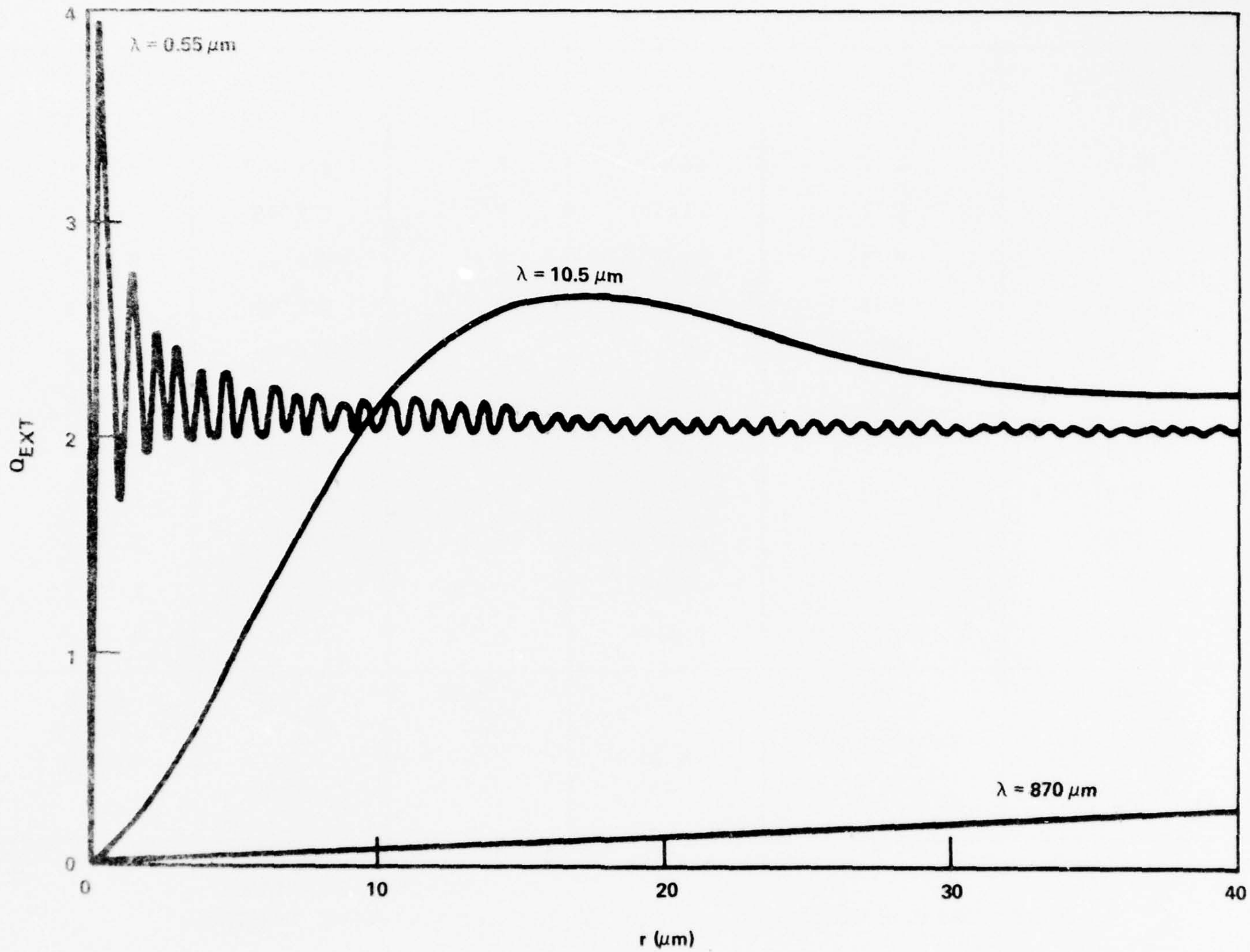

Figure 2. Q_{ext} versus r for 0.55, 10.5, and 870 μm.

TABLE 2. SAMPLE OF COMPUTATIONAL PROCEDURE FOR OBTAINING EXTINCTION COEFFICIENT

Radius Interval (μm)	$\overline{r_i^2}$ (μm^2)	N_i (cm^{-3})	$\pi \overline{r_i^2} N_i$ (km^{-1})	$\pi \overline{r_i^2} N_i Q_i$ for 0.55 μm (km^{-1})	$\pi \overline{r_i^2} N_i Q_i$ for 10.5 μm (km^{-1})
0 to 1	0.333	100.0	0.1047	0.23	0.01
1 to 2	2.333	55.5	0.4068	0.91	0.07
2 to 3	6.333	24.8	0.4934	1.11	0.18
3 to 4	12.333	3.1	0.1201	0.27	0.07
4 to 5	20.333	4.7	0.3002	0.65	0.25
5 to 6	30.333	4.4	0.4193	0.88	0.46
6 to 7	42.333	4.0	0.5320	1.12	0.72
7 to 8	56.333	7.6	1.3450	2.84	2.12
8 to 9	72.333	4.2	0.9544	2.01	1.72
9 to 10	90.333	3.0	0.8514	1.78	1.70
10 to 11	110.333	2.4	0.8319	1.72	1.80
11 to 12	132.333	1.1	0.4573	0.95	1.06
12 to 13	156.333	0.5	0.2456	0.51	0.60

TABLE 2. (Concluded)

Radius Interval (μm)	$\overline{r_i^2}$ (μm^2)	N_i (cm^{-3})	$\pi \overline{r_i^2} N_i$ (km^{-1})	$\pi \overline{r_i^2} N_i G_i$ for 0.55 μm* (km^{-1})	$\pi \overline{r_i^2} N_i Q_i$ for 10.5 μm* (km^{-1})
13 to 14	182.333	0.5	0.2864	0.59	0.72
14 to 15	210.333	0.3	0.1982	0.41	0.51
15 to 16	240.333	0.3	0.2265	0.47	0.60
16 to 17	272.333	0.3	0.2567	0.53	0.68
17 to 18	306.333	0.0	0.0000	0.00	0.00
18 to 19	342.333	0.0	0.0000	0.00	0.00
19 to 20	380.333	0.3	0.3585	0.73	0.94

*$\sigma(0.55) = 17.71\ km^{-1}$ and $\sigma(10.5) = 14.21\ km^{-1}$.

TABLE 3. SUMMARY OF MEASUREMENTS OF FOG DROPLET RADII

Source	Typical Radii (μm)	Maximum Radius (μm)	Miscellaneous Information
Arnulf et al. (1957)	2.5	15	France
Best (1951)	5 to 12	40	From earlier work by Hagemann
Cong and Dessens (1973)	8 to 10	22	Localized near plume from pulp mill
	4.5 to 5.2	17	Widespread through valley
Deloncle (1963)	<1	10	Urban, near Paris
	<0.75	8	Mountain top, France
Dickson et al. (1975)	3.4	118	Capistrano, California
Donaldson (1955)	10 to 25	100	Massachusetts
Eldridge (1961)	<1	32	Massachusetts
Findeisen (1932)	1 to 4	60	Hamburg, Germany
Garland (1971)	<1	40	Radiation fogs, all water
	10	70	Radiation fogs, ice crystals
	4	60	Advection fogs
Garland et al. (1973)	<0.6	20	Radiation fogs
Gathman and Larson (1974)	3 to 9	64	Greenland Sea
Gorchakov (1972)	5.5 to 12.5		Russia

TABLE 3. (Continued)

Source	Typical Radii (μm)	Maximum Radius (μm)	Miscellaneous Information
Grunow (1960)			Mt. Hohenpeissenberg, Germany
	1.5	7.5	Polar air
	4 to 7	12.5	Maritime air
	6 to 9	30	Continental air
Houghton and Radford (1938)	4 to 35	65	Typically advection fogs
Jiusto (1964)	5	17.5	Radiation
	10	32.5	Advection
Kozima et al. (1953)	2.5 to 7.5	55	Japan
Kumai (1973)	3.5 to 12.6	65	Point Barrow, Alaska; advection fogs
Kunkel (1971)	5 to 10	45	Otis Air Force Base
Low (1975)	9 to 13	21	Radiation fog, Ft. Rucker, Alabama
	4 to 13		Mixed radiation-advection, California
Ludwig et al. (1974)	0.1	15	Radiation fog
Mack et al. (1973)	4 to 8	31	At sea

TABLE 3. (Continued)

Source	Typical Radii (μm)	Maximum Radius (μm)	Miscellaneous Information
May (1961)	<0.5 to 15	160	Salisbury Plain, England
Mészaros (1965)			Budapest, Hungary
	<0.4 to 10	43.8	Radiation
	2 to 13	101.5	Advection
Okita (1962)	6 to 17	60	Radiation fogs in Japan
Pedersen and Todsen (1960)			Oslo, Norway
	<2	16	Radiation
	2	25	Advection
Pilié et al. (1975)	3 to 12	31	Chemung River Valley, New York
Reinking (1975)	3	7.5	San Joaquin Valley, California
Roberts (1976)	0.2 to 1.1	8	Grafenwöhr, Germany
Rogers et al. (1974)	8	115	California coast
Rozenberg (1974)	5		Thin
	50		Medium
Tag (1976)	8	23	Panama Canal Zone

TABLE 3. (Concluded)

Source	Typical Radii (μm)	Maximum Radius (μm)	Miscellaneous Information
Tampieri and Tomasi (1976)	8	22	Radiation fog, Italy
Thompson et al. (1967)	10	34	Otis Air Force Base
Thuman and Robinson (1953)	40		Ice prisms
	32		Ice hexagons
	15		Ice droxtals
Tverskoi (1965)	1.5	60	Radiation fog
	2	60	Evaporation fog
Webb (1956)	5 to 19	70	Washington, D.C. and Virginia

optical densities were 10 to 15 times larger in the visible than at 10 μm. In fogs which they called selective fogs atmospheric extinction of visible wavelengths varied from about 2 to over 20 times the extinction at a wavelength of 10 μm. In evolving fogs, visible wavelengths were attenuated from about 1.4 to 20 times the wavelength of 10 μm. In stable fogs the 10-μm attenuation was always at least half the visible attenuation, and in some stable fogs attenuation at 10 μm was almost as much as in the visible.

Best (1951) discussed a paper published by Hagemann (1936) from Hamburg, Germany, but Best's paper is probably more readily available. The peaks of the drop-size distributions illustrated in Hagemann's Figure 6 were typically from about 5- to 12-μm radius. Maximum drop sizes measured by Hagemann were near 40 μm, and most samples contained a considerable number of drops with radii greater than 10 μm. The samples in Hagemann's original articles showed that many distributions were multimodal, and this was unfortunately lost in Best's parameterization.

Bimodal and multimodal distributions have also been inadequately parameterized by most other investigators. Essenwanger (1976) pointed this out in his discussion of Mallow (1975). Rensch and Long (1970), Baronti and Elzweig (1973), and Tampieri and Tomasi (1976a, b) also used distribution functions which allowed only a single mode.

Cong and Dessens (1973) made measurements in France on the upper Garonne River near a pulp mill which ejected 65 tons of water vapor per hour into the atmosphere. Measurements were made in a valley where wind speeds were light or it was calm, and there were frequent inversions. They studied two fogs which were spread throughout the valley basin and two fogs which were localized in the vicinity of the falling from the plume emitted by the pulp mill. Drops were larger in the localized fogs which had mean radii of 8 and 10 μm. Maximum radii were about 22 μm. Mean radii in the more widespread fogs were 4.5 and 5.2 μm, and maximum radii were about 17 μm. In both cases, large numbers of drops had radii greater than 10 μm.

Deloncle (1963a, b) studied fogs near Paris and on a mountain, Puy-de-Dôme, in France. Near Paris, most drops had radii less than 1 μm; the maximum radius was about 10 μm. Some of these distributions were bimodal (see Figure 5 of Deloncle, 1963a) with a secondary maximum near 5.5 μm. Deloncle found smaller drops on the mountain Puy-de-Dôme. Maximum radii were about 8 μm, and the largest number of drops had radii less than 0.75 μm. Even the secondary modal radius was only about 1.5 μm.

Dickson et al. (1975) made extensive measurements at Capistrano Test Site in California. Most of the data were in the form of computer printouts, but a typical example of fog was discussed in Volume I. The maximum radius of drops measured in this example was 118 μm, but most drops had radii less than 82 μm. The main modal radius was about 3.4 μm, and there were very small secondary modes at 9.4, 12.6, and 19.4 μm. Other fluctuations appeared to be too small to consider significant. The liquid water content was about 0.17 g/m^3.

Donaldson (1955) made measurements near Buzzard's Bay in Massachusetts. According to Donaldson's Figure 6, volume mean radii in his samples varied from 16 to about 35 μm. Therefore, the linear mean radii probably varied from about 10 to 25 μm. From Donaldson's Figure 2, one sees that no large secondary modes were apparent, and the maximum drop-size was about 2.8 times the volume mean. It follows that the maximum drop-size must have been near 100-μm radius. Liquid water contents varied from about 0.013 to 0.16 g/m^3.

Eldridge (1961) found that in 11 of 14 samples the number of drops increased monotonically as the droplet radius decreased. The smallest drop-size class in Eldridge's Tables 2 and 3 was 0.5- to 1-μm radius. The largest class was for radii from 16 to 32 μm. In 2 of the 14 samples, the mode was in the 1- to 2-μm class; one sample had the mode in the 2- to 4-μm class. The liquid water content varied from 0.039 to 0.365 g/m^3.

Findeisen (1932) measured drop-size distribution in fogs in Hamburg, Germany. All the samples illustrated in Findeisen's Figures 6 and 7 had large numbers of small drops and were multimodal. There were large numbers of drops with radii greater than 10 μm. The five distributions in Findeisen's Figure 7 had at least one small secondary maximum with these larger radii. The maximum radius was about 60 μm.

Garland (1971) had 25 sets of measurements in a table. The fogs were classified according to whether they were judged to be radiation fogs or advection fogs. Most calculated visual ranges were a little more than observed visual ranges and, perhaps, some small drops were missed. In radiation fogs with no ice crystals, droplet radii varied from 0.3 to 40 μm. In a radiation fog which consisted entirely of ice, the radii varied from 6 to 70 μm. In advection fogs the radii varied from 0.4 to 60 μm. Garland's table did not give a typical or average radius, but I have estimated values from the information which was

given and from the graphs. Most drops apparently had radii less than 1 μm in the liquid radiation fogs. Ice fogs had typical radii greater than 6 μm, probably at least 10 μm. Advection fogs on the graphs in Figure 3 had typical radii from 2 to 8 μm. Liquid water was in the range of 0.023 to 0.173 g/m^3.

Garland et al. (1973) studied only radiation fogs. In five out of six samples the largest drops had radii of about 15 μm; one sample had a drop with a radius as large as 20 μm. In five out of six samples the category containing the most drops was less than 0.6 μm. Large secondary modes did not occur. The liquid water content varied from 0.05 to 0.21 g/m^3.

Gathman and Larson (1974) observed many atmospheric variables in three fogs in the Greenland Sea. They believed that their method of measurement was 100% efficient in collecting particles with radii greater than 1.0 μm. Median radii in their 15 fog samples varied from 3 to 9 μm according to their Table 2. Their graphs were hard to read, but maximum drop radii apparently varied from about 32 to 64 μm in their Figures 8, 9, and 10. Calculated liquid water contents were in the range of 0.041 to 0.251 g/m^3.

Gorchakov et al. (1972) made assumptions about the fog drop-size distributions and used an optical scattering technique to estimate the parameters in the distribution function for three cases. In two cases the modal radius was about 5.5 μm. They were surprised that in the third case the mode was near 12.5 μm, and the particle size distribution was quite narrow compared to the other two cases.

Grunow (1960) investigated fogs on Mt. Hohenpeissenberg in upper Bavaria in Germany. He found that cold polar air was characterized by droplets from 1- to 7.5-μm radius. Warm maritime air masses normally had droplets with radii from 2 to 12.5 μm. Maritime air masses with a long continental trajectory had droplets from 2.5 to 30 μm. Typical droplets in these three kinds of air masses had radii of 1.5, 4 to 7, and 6 to 9 μm, respectively.

Houghton and Radford (1938) studied advection fogs at Round Hill in South Dartmouth, Massachusetts. They obtained 40 volume distribution curves in 16 fogs having peaks from 6- to 45-μm radius. The range of radii was from 1 to 65 μm. Because the linear mean of radii is less than the radius of a droplet of mean volume, typical radii were probably from about 5 to 35 μm. The largest liquid water content was about 0.3 g/m^3.

Jiusto (1964) summarized a literature survey and divided fogs into two main types: radiation and advection. He assumed that inland fogs were radiation fogs and that coastal fogs were of the advection type. The average radius of radiation fog droplets was 5 μm, and the maximum was about 17.5 μm. The liquid water content was about 0.11 g/m^3. The larger advection fog droplets had an average radius of about 10 μm and a maximum near 32.5 μm. The liquid water content of advection fog was assumed to have an average of about 0.17 g/m^3. Jiusto (1974), in a later article, has pointed out that these simplified numbers represent only typical values that will vary considerably in individual cases and with local conditions.

Kozima et al. (1953) divided the fog drop-size distributions that they measured in Hokkaido, Japan into four groups. Fogs containing particles with radii greater than 30 μm were type D. Type D typically had the largest number of particles in the smallest size category, and the number of particles decreased monotonically with increasing size. In type A fogs, 70% of the particles had radii less than 5 μm. In type B fogs, less than 70% of the drops had radii less than 5 μm and less than 35% had radii greater than 10 μm. More than 35% of the drops had radii greater than 10 μm in type C fogs, but none had radii greater than 30 μm. The largest radii measured by Kozima et al. were 55 μm.

Kumai's (1973) investigation of advection fogs in Point Barrow, Alaska, found maximum radii of 65 μm. The categories with most drops varied from 3.5- to 12.6-μm radius. Observed visibilities were slightly smaller than computed visibilities; therefore, some small drops were missed. In Figure 5 of Kumai's article, visibility was plotted versus liquid water content. There was a lot of scatter in the data, and the long-lasting fogs showed far more scatter than the short-period fogs. When visibilities were 1 km or less, the amount of liquid water varied from 0.033 to 0.15 g/m^3.

Kunkel (1971) used a laser hologram camera to measure drop sizes in fogs. During part of the test, his instrument would only measure large drops. A cascade impactor was used to fill in additional data. During the remainder of the test, droplets with radii as small as 2 μm could be measured. Kunkel's Figure 3 indicated that radii near 45 μm were measured. From his Figure 4, which represented measurements made entirely with one type of instrument, one sees that typical radii were from 5 to 10 μm. The number of grams of liquid water varied from 0.021 to 0.148.

Laktionov et al. (1973) studied statistical characteristics of fog in Russia. They found that the number of droplets with radii less than 8 μm was negatively correlated with the number of droplets with radii greater than 12 μm. For example, the number of droplets with radius 18 μm had about a -0.4 correlation with the number of droplets with a radius of 0.45 μm. If this should be true in other locations, one would not have to worry that numerous small drops were missed by the measurement technique in fogs with large numbers of large drops. The discussion in Section II of the present report also indicates that small drops contribute much less to extinction than large drops.

Low (1975a) reported on two sets of measurements. The first was done by Dickson at Skelly Field near Ft. Rucker, Alabama. This fog was the radiation type. The wind varied from calm to about 1 m/sec throughout most of its existence. Typical radii were from 9 to 13 μm, and maximum radii were about 21 μm. Liquid water content at Skelly Field varied from 0.14 to 0.21 g/m^3.

The second set of measurements reported by Low were in Redwood Valley near Arcata, California. These measurements were made by Bonner and White, but Low has included corrections to errors which were found in their orginial work. The Redwood Valley fogs were of a mixed radiation-advection type but Low believed that they were predominately radiational. Typical radii were from 4 to 13 μm. Information about the maximum radii in the Redwood Valley fogs was not given. The maximum liquid water content was 0.65 g/m^3 and the minimum was 0.04 g/m^3.

Ludwig et al. (1974) measured droplet size distributions in radiation fog at Brannan Island State Park in the delta of the San Joaquin and Sacramento Rivers. According to their Figures 12 and 24 the largest number of particles were the smallest ones less than a few tenths of a micrometer in radius, and the maximum radius was about 15 μm.

Mack et al. (1973) measured fog parameters at sea near Monterey, California, and near the Farallon Islands. Figures 5 and 6 of their report contained many histograms of drop-size distributions. The peaks typically occurred at radii from about 4 to 8 μm, and most drop sizes were in the range of 2- to 16-μm radius. Several distributions were multimodal. The largest radius shown on the graphs was about 31 μm. Drizzle occurred during the two most thoroughly studied fogs. It was qualitatively estimated that droplet radii were as large as 100 μm. The maximum liquid water content was 0.18 g/m^3.

May (1961) studied 28 fogs. The method of measurement discriminated against very large and very small droplets. May believed that one could not place an upper limit on the size of a fog droplet because the spectrum merged continuously into that of drizzle or rain when it accompanied a fog. In any case, May's Table 2 indicated a range of droplet radii of 0.25 to 160 μm. In 9 of the 28 fogs the maximum droplet radius was greater than 53 μm and in 11 fogs the maximum radius was less than 28 μm. Other characteristics of the fogs showed a wide variation even though all measurements were taken from the same position on the side of a building on open Salisbury Plain in England. One sample had a minimum radius of 8 μm, and another sample had a maximum radius of 7.5 μm. Three distributions had a median radius less than 0.5 μm but a maximum radius greater than 32 μm. One sample had a median radius of 15 μm. Liquid water contents which were obtained by weighing varied from 0.0044 to 0.27 g/m^3. Magnitudes computed from the drop-size distributions ranged from 0.0043 to 0.297 g/m^3.

Mészaros (1965) studied 26 radiation fogs and 13 advection fogs in Budapest, Hungary. Mészaros' Tables I and II listed a great deal of information about each fog, including mode radius, mean radius, mean square radius, mean volume radius, and maximum radius. In the 26 radiation fogs the mode radius varied from less than 0.4 to 10.2 μm, and the mean radius varied from 3.7 to 10.6 μm. Maximum radii in the radiation fogs were in the range from 18.5 to 43.8 μm. Mean liquid water content in the radiation fogs was 0.062 g/m^3. Average droplets in the 13 advection fogs were larger than the radiation fog droplets. The principal modal radius varied from 2.1 to 12.9 μm. Two advection fogs were bimodal, and in one of these the secondary mode was at 28.0 μm. Mean radii were from 2.2 to 17.0 μm in the advection fogs. Maximum radii in the advection fogs varied from 31.5 to 101.5. In the advection fogs the average liquid water content was only 0.022 g/m^3, much less than in the radiation fogs.

Okita (1962) examined drops in four radiation fogs in Hokkaido, Japan. Okita made measurements from the surface to 250 m. The largest drops near the surface had radii of 60 μm. Mean radii varied from 6 to 17 μm according to Okita's Figure 20. The maximum liquid water content was about 0.4 g/m^3 near the surface.

Pedersen and Todsen (1960) measured fog droplet sizes near Oslo, Norway. The fogs classified as radiation fogs had maximum radii of about 16 μm, and advection fog droplets had radii as large as 25 μm. Typical distributions of both kinds of fog were bimodal, and one mode was from 5 to 7 μm. In radiation fogs, one mode was typically less than 2 μm, and in advection fogs one mode was near 2 μm.

Pilié et al. (1975a, b) made extensive micrometeorological measurements in 11 fogs in the Chemung River Valley near Elmira, New York. Measurements were made aloft as well as near the surface. The broadest drop-size distributions always occurred near the surface. Deep fog formed first aloft with its base 30 to 60 m above the surface, but ground fog a few meters thick could result from diffusion of heat to the cold ground. The temperature distribution leading to the formation of a deep valley fog appeared to be the result of nocturnal valley circulations. Further radiative cooling of the fog top produced an unstable lapse rate, and subsequent turbulence caused the fog base to propagate downward to the surface. Typical radii were from 3 to 12 μm, and the maximum radius was about 31 μm. Most distributions in mature fog at the surface were very broad and multimodal. The average liquid water content at the time of minimum visibility was 0.1 g/m^3.

Reinking (1975) studied warm radiation fogs under calm conditions in the San Joaquin Valley in California. Maximum radii were about 7.5 μm, and typical mean radii were near 3 μm. Detailed information was not given.

Roberts (1976) obtained drop-size distributions from Grafenwöhr, Federal Republic of Germany. Roberts' Figure 1, which showed plots of five drop-size distributions, did not indicate that there were any particles with radii greater than 8 μm. Most of the distributions had a maximum near the smallest size shown on the curves, about 0.2 μm. One of the distributions had a maximum at slightly more than 1 μm and a secondary maximum at about 7.25 μm. Roberts' Figure 5 showed that even the small variation in drop-size distributions produced measurable changes in extinction for liquid water contents appropriate to moderate and light fog and mists, although the observations were quite close together for very large liquid water contents and for relatively clear air. For example, for a liquid water content of about 0.007 g/m^3, extinction of the 10-μm wavelength of energy varied by about a factor of 3, and for about 0.08 g/m^3 extinction varied by a factor of 2. Observations were scarce near 0.03 g/m^3.

Rogers et al. (1974) investigated the life cycle of California coastal fogs about 1 nmi inland near Vandenberg Air Force Base. The range of radii was typically 1.5 to 115 μm, and the mean radius at a height of 1.2 m was 8.4 μm according to their Table III. Graphical data were not given for 1.2 m but only for heights of 13 m and higher. At the higher levels the distributions tended to peak at about 5- to 7-μm radius. The average liquid water content was 0.08 g/m^3, and the maximum was 0.12 g/m^3 at the 1.2 m height.

Rozenberg (1974) has summarized expected mean drop sizes for different hydrometeors on page 279 in Table 6.14 of the English translation of the Russian report. The mean droplet radius was 5 μm in thin fogs and 50 μm in medium fogs.

Tag (1976) discussed earlier work which was based on data taken in the Panama Canal Zone. Tag's Figure 2 indicated a maximum radius of about 23 μm. Typical radii would be less than the volume mean radius of 10.8 μm. The liquid water content was 0.39 g/m^3.

Tampieri and Tomasi (1976a) have fit various drop-size distributions to a modified gamma function. A report describing a study by Vittori and Pesaresi at Baricella in the Po Valley in Italy was among the published work which they discussed. Maximum drop radii were about 22 μm and typical radii were about 8 μm in the fogs in the Po Valley. Tampieri and Tomasi classified these fogs as radiation fogs.

Thompson et al. (1967) have described a laser hologram camera system for measuring drop sizes. Their article contained one sample histogram of data taken at Otis Air Force Base, Massachusetts. Typical radii were near 10 μm, and the maximum radius was about 34 μm.

Thuman and Robinson (1954) studied Alaskan ice-fog particles. The highest temperature at which ice-fog occurred was -30°C during the winter of 1952-1953 at Eielson Air Force Base. Thuman and Robinson were primarily concerned with crystal size as a function of temperature. The minimum size appearing in their Figure 7 was about 13 μm.

Tverskoi (1965) classified fogs as radiation and evaporation fogs in Figure 107, page 324, of the English translation. Two radiation fogs had modal radii between 1 and 2 μm. The graphs showed one radiation fog to have a maximum radius of about 5.5 μm and the other a maximum of 11.5 μm. The modal

radius of the evaporation fog was about 2 μm and the maximum about 10 μm. However, Tverskoi stated on a later page that the maximum radii in the fogs were about 60 μm.

Webb (1956) gave three representative drop-size distributions in his Figure 4. The radiation fog at Pimmit Green, Virginia, had a modal radius of about 5 μm, but the graph was hard to read and the maximum radius was uncertain. Information in the figure caption about the two curves from Washington, D.C., was not consistent with information in Webb's Table 1. One distribution had a modal radius near 7.5 μm and few drops had radii larger than 11 μm. The other curve was distinctly bimodal with peaks at 14 and 19 μm radius. This distribution with the large drops was probably the advection fog. It had more drops with radii greater than 20 μm than with radii less than 10 μm. The maximum radius was near 70 μm. Webb stated that although droplets of 0.3 μm radius could not be seen with certainty, droplets with radii of 0.75 μm were easy to measure by his technique.

In spite of the large amount of work that has been done in measuring fog drop-size distributions, more studies are needed.

It is obvious that in some locations the nature of fog drop-size distributions can change drastically from one time to another. This has been shown very clearly by Grunow (1960), May (1961), and Mészaros (1965). Therefore, the reader is cautioned against assuming that any values in Table 3 are always valid for the specified location. However, there may be places where the life cycle of a fog is almost always similar, but systematic measurements over a period of years will be necessary to demonstrate this.

It should also be noted here that changes in fog characteristics can have very small space and time scales. Richer (1970) found appreciable changes in propagation at 140 GHz (2142 μm) within a fog during a time when no apparent changes in visibility occured. In Richer's experiment, attenuation increased from 15 to 23 dB/km in a 30-sec period and then decreased to 15 dB/km during the following 30 sec. Zuev et al. (1972) probed a fog with a 0.6943-μm laser. Oscillogram traces of reflected signals showed rapid fluctuations indicating that the inhomogeneities of the fog were in constant motion. George (1972) studied a fog in Washington, D.C., and the length of most elements fell within the range of 50 to 100 ft. Chisholm and Kruse (1974) made mesoscale measurements of visibility at L. G. Hanscom Field in Massachusetts. They found that temporal and spatial variability was much greater in radiation fogs than in advection fogs.

A few investigators have discussed the variation of drop-size distributions during the life cycle of a fog. Pilié et al. (1975b) made one of the most thorough studies of the life cycle of valley fog. They found that shallow ground fog usually occurred before the formation of deep valley fog. The ground fog had mean radii of 2 to 4 μm and a range of 1 to 10 μm. As deep fog formed aloft, mean radii near the surface increased to 6 to 12 μm. Small droplets occurred again at the first visibility minimum after which a bimodal distribution developed at the surface in about half of the fogs. One mode was at a radius of 2 to 3 μm and the other between 6 and 12 μm. Pilié et al. found no consistent change in the shape of drop-size distributions during fog dissipation, but Laktionov (1967b), in a study near Moscow, found that the number of larger drops decreased during fog dissipation. However, Dickson and Hales (1963) have made theoretical computations of visibility changes based upon the assumption that droplets become larger as fog ages. Dickson and Hales did not specifically state that this behavior carried through to the final dissipation stages; their belief was based primarily upon the laboratory part of Findeisen's (1932) study. Low (1975a) examined the life cycles of one radiation fog and four mixed radiation-advection fogs. In the radiation fog, the mean and median radii increased with time from the formative stage to the end of the mature stage and then decreased slightly during dissipation. Behavior was not consistent among the four mixed radiation-advection fogs.

Another characteristic of fogs which has aroused interest is the liquid water content. Many people, including Eldridge (1971) and Barteneva and Polyakova (1965), have suggested that liquid water content should be a simple function of visibility. However, Barteneva and Polyakova's own data in their Figure 2 showed a lot of scatter. Eldridge considered possible observational errors in only two sets of data to conclude that they should be very close together. Koester and Kosowsky (1970) suggested using two relationships: one for radiation fog and one for advection fog. This oversimplification had the merit of illustrating very clearly the pitfall of casually using any equation one might find in the literature. They suggested maximum liquid water contents of 1.0 and 0.4 g/m^3 for radiation and advection fogs, respectively. The earlier part of this section of the present report indicates that most fogs have a liquid water content less than 0.4 g/m^3. Roberts (1976) measured values slightly more than 1.0 g/m^3. Low (1975a) reported 0.65 g/m^3 with a visibility of 84 m. In industrial regions of Bohemia in Czechoslovakia Anyz (1964) measured liquid water contents greater than 0.5 g/m^3 with visibilities in excess of 100 m. This could only occur if there were many large drops. Anyz measured 0.606 g/m^3 a short time after the last visibility measurement.

The preceding discussion applies to observations near the surface. Very few observations exist for higher levels, but in one case Okita (1962) observed a liquid water content of 1.6 g/m^3 at a height of 50 m. Rogers et al. (1974) also found that average and maximum liquid water content increased with height, but at 42 m the largest measured liquid water content was only 0.4 g/m^3. Stalenhoef (1974) found that slant visibility from 40 m was normally less than horizontal visibility at 2 m.

Finally, the reader is urged to remember that a few large drops can make a bigger contribution to extinction than many small drops as has been illustrated in Table 2. This is particularly true at 10.5 μm, where extinction is comparable to visible extinction for particles with radii greater than 10 μm. Therefore, the typical radii in Table 3 must not be considered alone without reference to the number of large drops. A maximum radius greater than 30 μm was usually an indication of a significant number of large particles.

IV. COMPARISON OF EXTINCTION OF DIFFERENT WAVELENGTHS

Drop-size distributions were taken from six articles. Kumai (1973) and Eldridge (1966) listed data in convenient tabular form. Thirteen of the distributions from Kumai were associated with visibilities less than 1 km and thus came within the definition of fog used in this report. Kumai's fogs typically contained 20 to 40% of radii greater than 10 μm, and no radii were less than 2.85 μm. Eldridge's 12 fog drop-size distributions had no radii greater than 8 μm, and most were less than 1 μm. Pilié et al. (1975b) and Pedersen and Todsen (1960) provided graphs which were fairly easy to read. Typically, over 10% of radii from Pilié et al. were greater than 10 μm, but only a few percent from Pedersen and Todsen were greater than 10 μm. Data were taken from 27 graphs of mature fogs of Pilié et al. and from 3 graphs of Pedersen and Todsen. Garland (1971) and Garland et al. (1973) provided graphs which were difficult to read, but they did provide some supplementary information in tables. Five drop-size distributions were used from each article, and the droplets were typically small. Altogether, extinctions were computed for 65 drop-size distributions.

Figures 3 through 7 illustrate the results of computations made with the 65 drop-size distributions according to the procedure described in Section II.

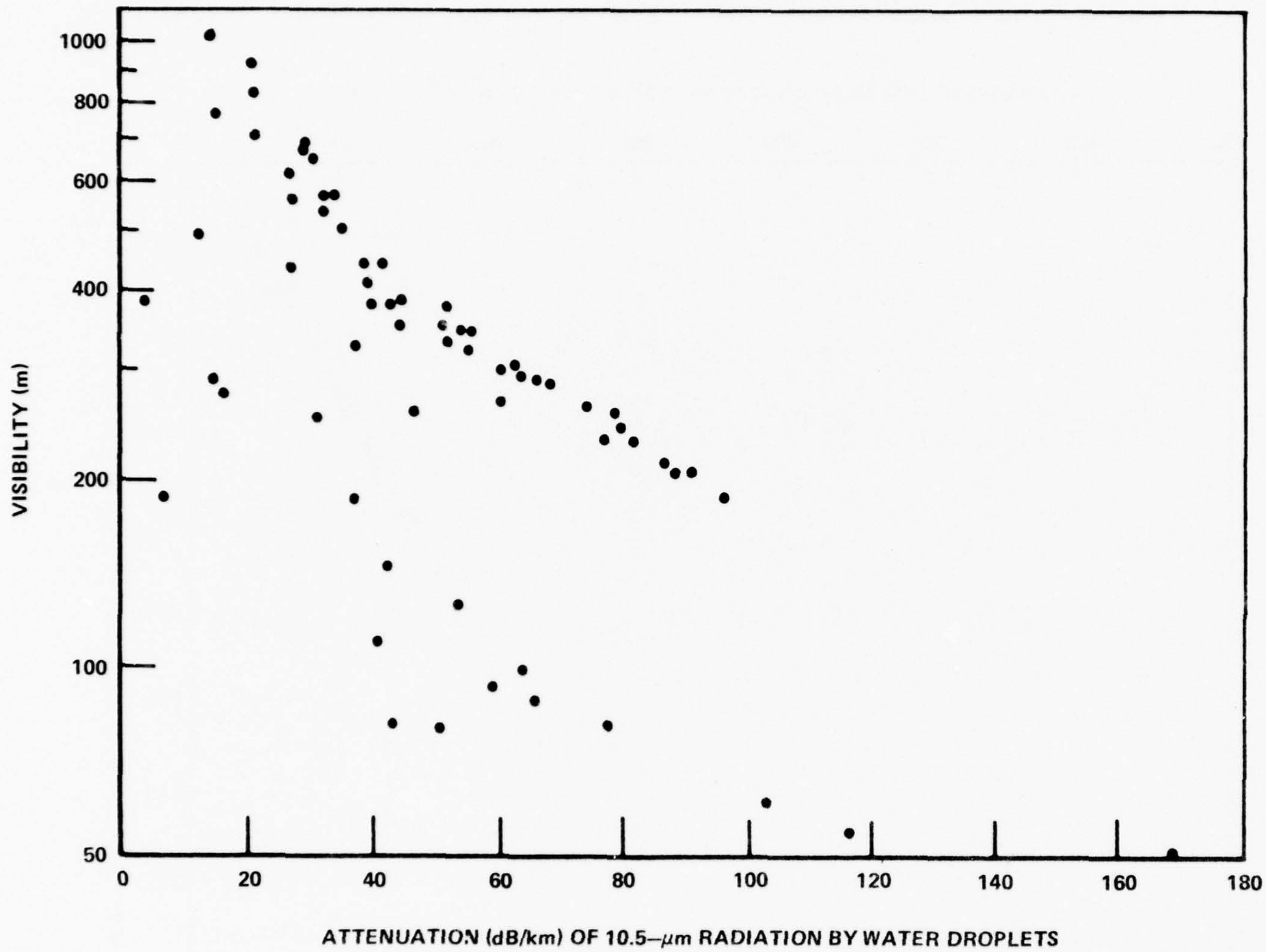

Figure 3. Plot of visibility versus attenuation at 10.5 μm.

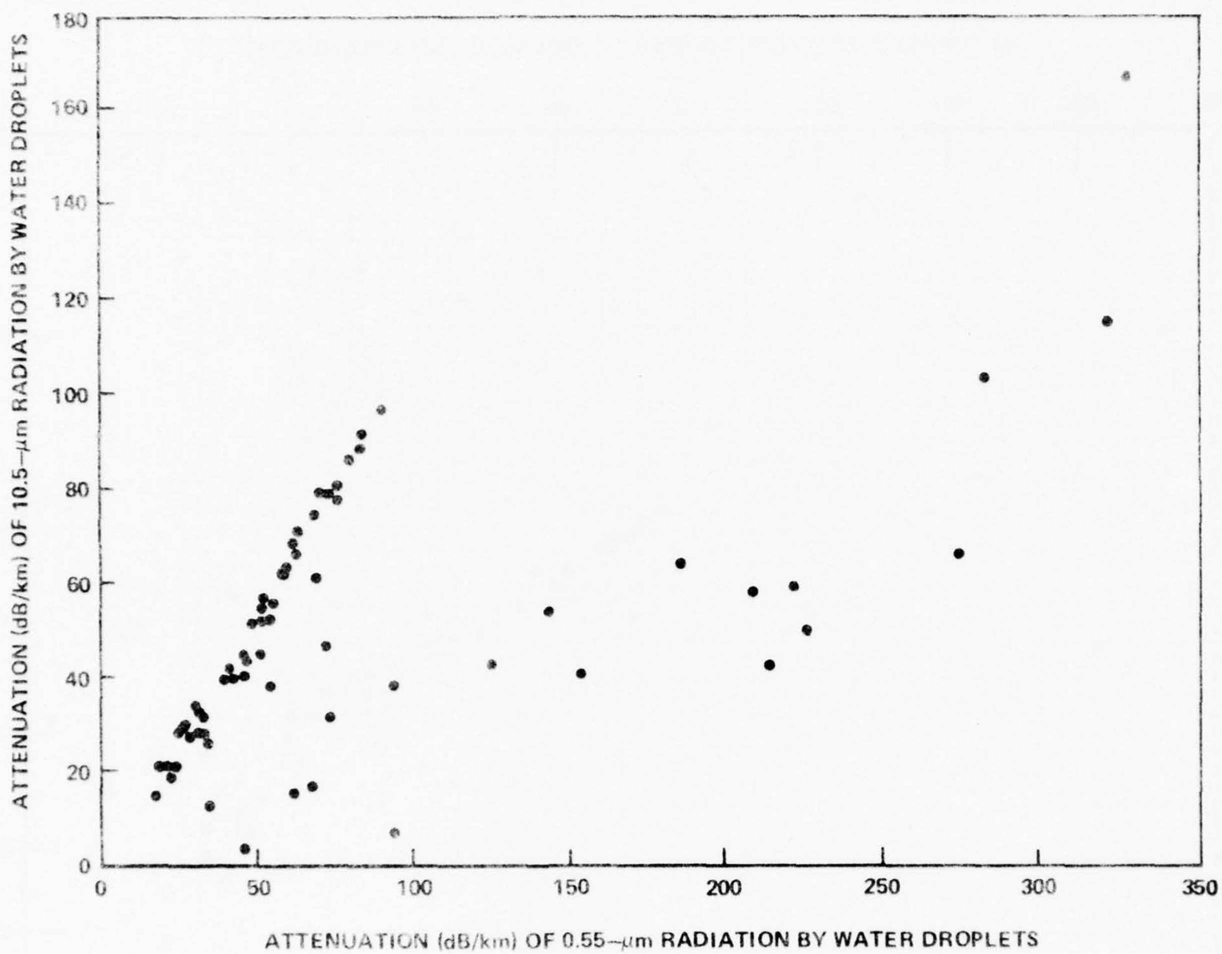

Figure 4. Comparison of attenuation of 10.5- and 0.55-μm radiation by fog droplets.

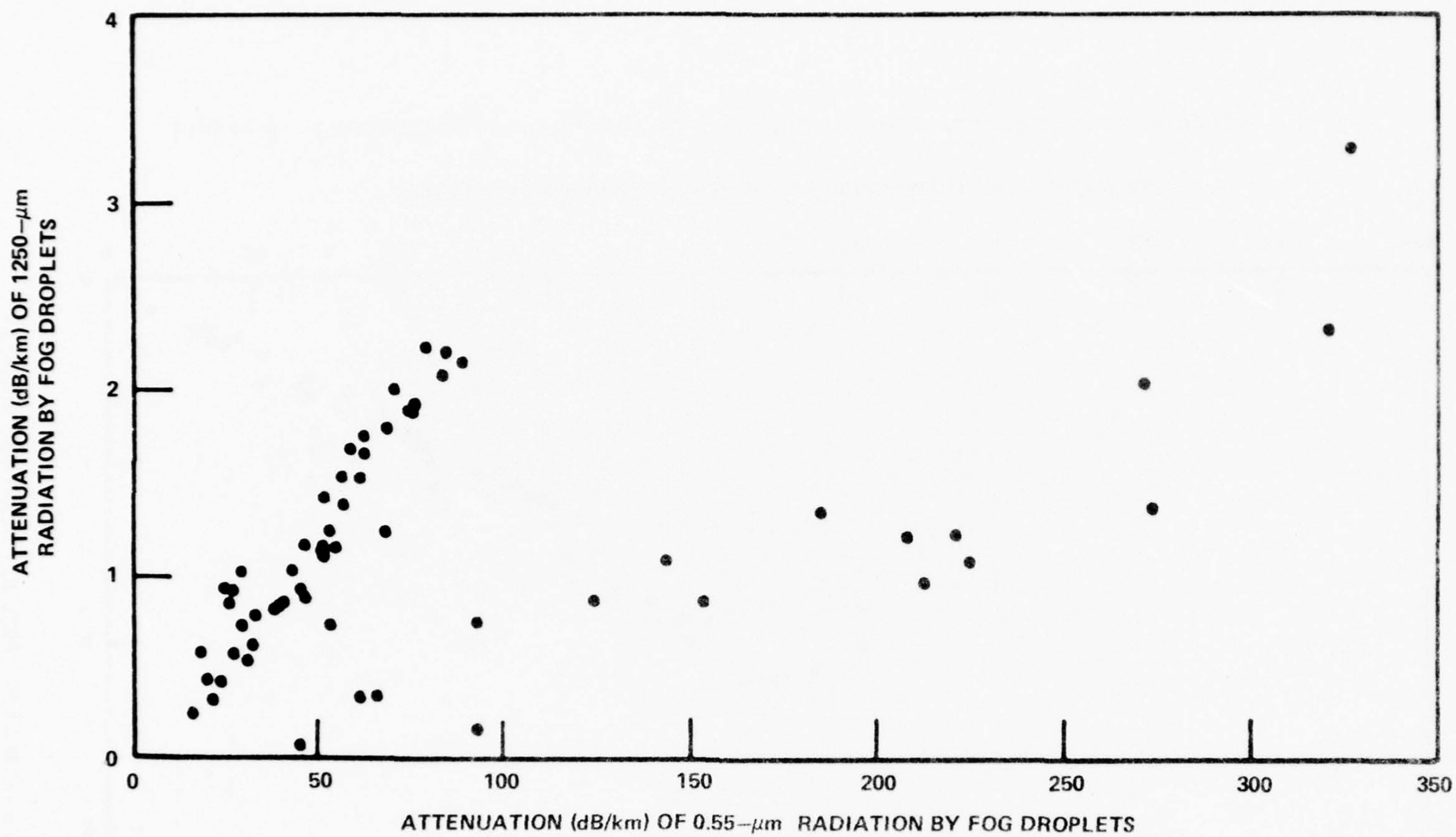

Figure 5. Comparison of attenuation of 1250- and 0.55-μm radiation by fog droplets.

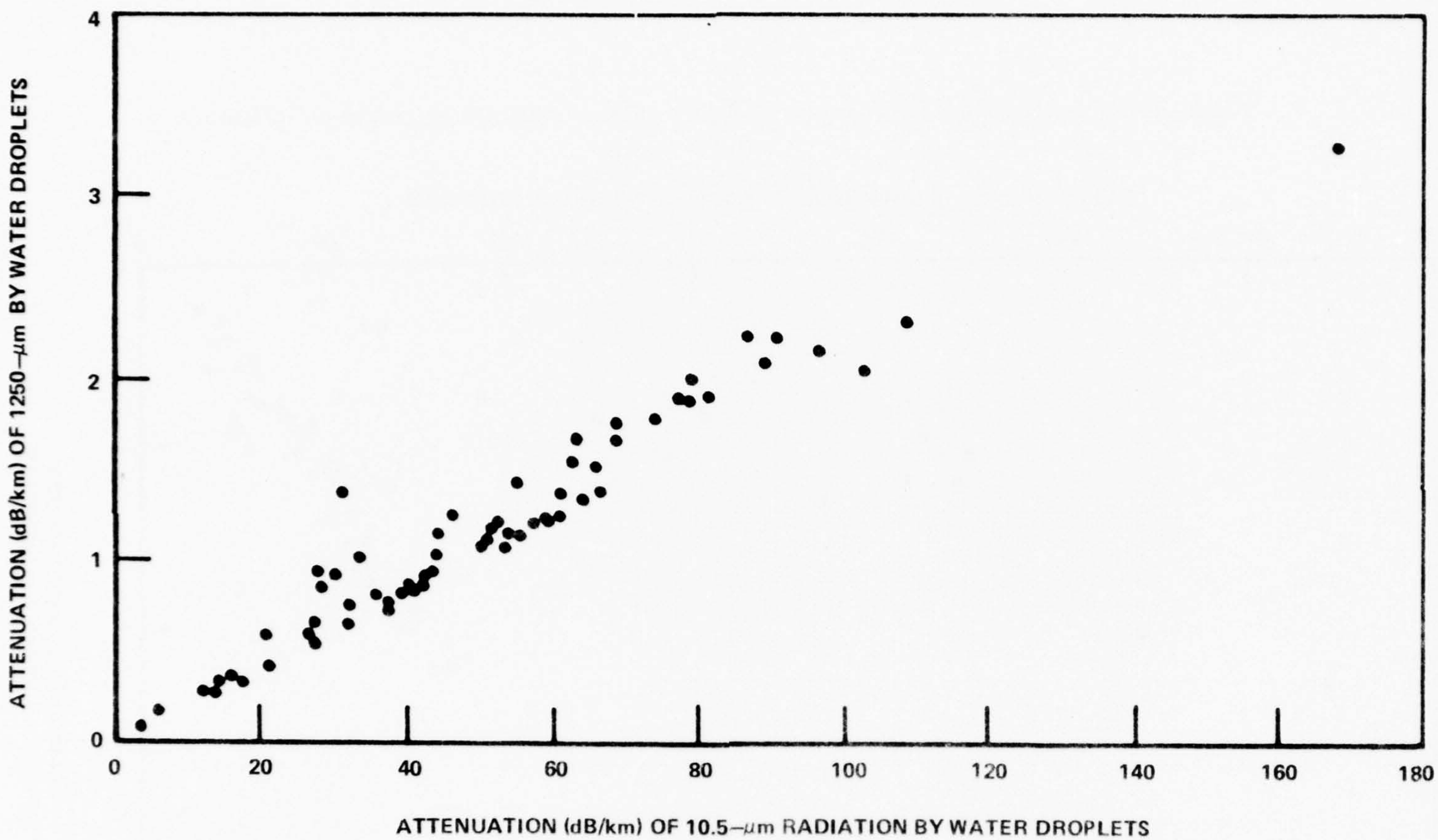

Figure 6. Comparison of attenuation of 1250- and 10.5-μm radiation by fog droplets.

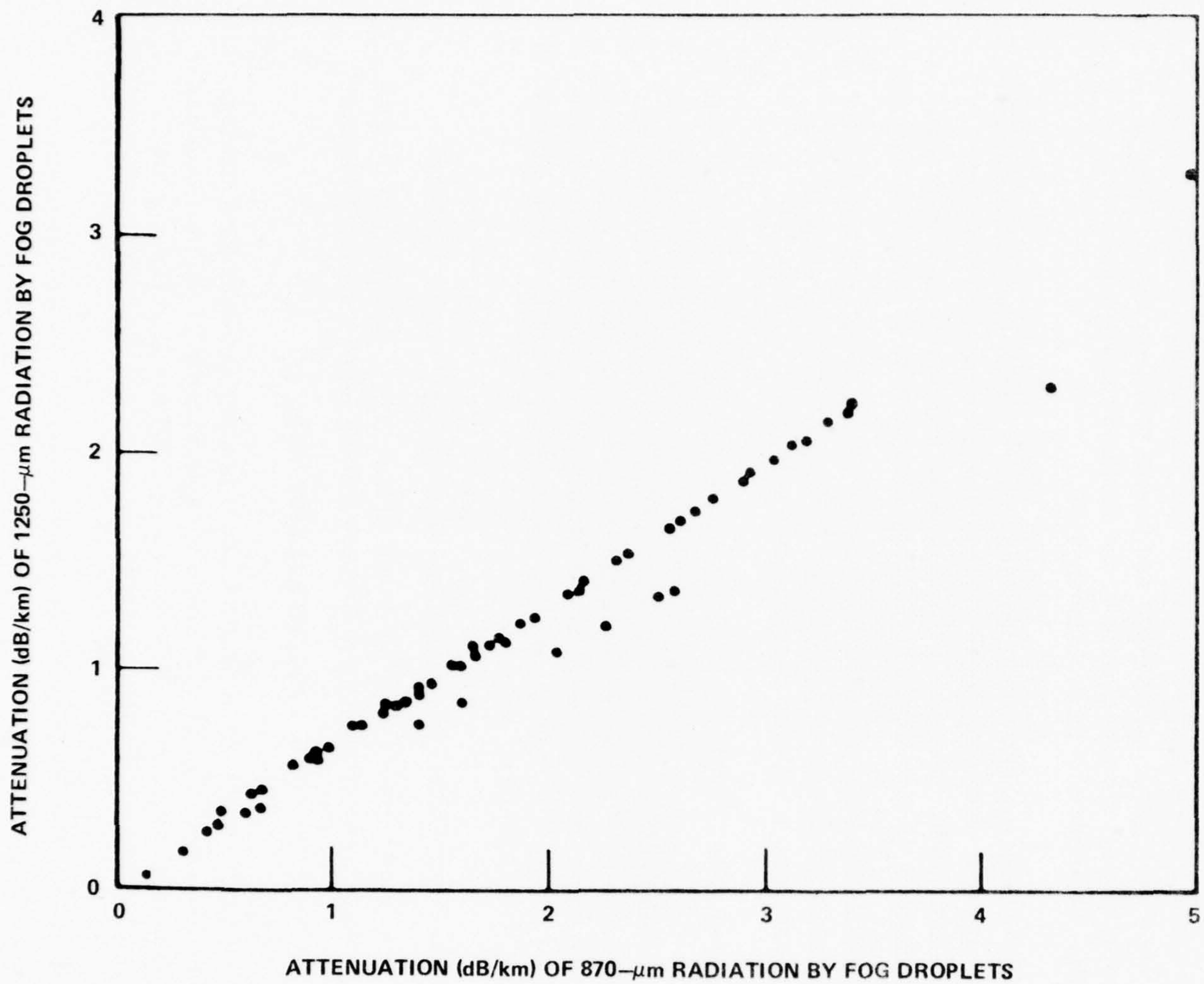

Figure 7. Comparison of attenuation of 1250- and 870-μm radiation by fog droplets.

Figures 3 and 4 show the relation between attenuations of visible and infrared energy. Figure 3 is a plot of visibility as a function of attenuation at 10.5 μm. There is obviously a great deal of scatter in the data. An attenuation of 50 dB/km at 10.5 μm can be associated with visibilities considerably less than 100 m or over 300 m. If the data are plotted with both axes in units of decibels per kilometer as in Figure 4, the scatter is still obvious. The correlation of the data in Figure 4 is only 0.61.

Before comparing these data with the work of others one should consider the following facts. The index of refraction of water does not vary much throughout the visible. Except for the very small drops with radii less than 3 μm, the mean Q_{ext} over a reasonable drop-size interval is about the same for different visible wavelengths. The index of refraction of water at 10.5 μm is close to that for wavelengths from 10.0 to 10.6 μm, and the parameter $\alpha = 2\pi r/\lambda$ does not vary a lot over this wavelength interval.

Bisyarin et al. (1971) made comparisons of attenuation at 10.6 μm with attenuation at 0.63 μm in real and laboratory fogs. The mean ratio of attenuation at 10.6 μm to attenuation at 0.63 μm was 0.38 for several real fogs and 0.43 for laboratory fogs. It was indicated that about 15% of their ratios were less than 0.20 and about 15% were greater than 0.60 in the real fogs. Sample data in their Figure 5 showed that they were including visibilities greater than 1 km under their definition of fog.

Chu and Hogg (1968) plotted a graph of wavelength versus expected attenuation by fogs with 0.1 g/m^3 of liquid water. Their estimate for 10.5 μm was 50 dB/km. Some of the fogs in Figures 3 and 4 which attenuated 10.5 μm about 50 dB/km had a liquid water content near 0.1 g/m^3.

Donati (1973) considered the problem of imaging through hazes and fogs. Calculations indicated that for high visibilities penetration of fog by 10 μm was much greater than penetration by visible energy. Under conditions of low visibility, the infrared offered only modest improvement over the visible.

Johnston and Burch (1967) measured the ratio of 10.0-μm attenuation to 0.546-μm attenuation in artificial fogs in the laboratory. Ratios were measured from 0.54 to 0.79 according to their Table II.

Rensch and Long (1970) used a model of fog drop-size distribution for theoretical computations. It was found that when the radius of drops with the maximum number density was greater than 5 μm, the extinction coefficient became wavelength independent for wavelengths from 0.34 to 10.6 μm. In my computations, most of the distributions with the radius of maximum number density greater than 5 μm had 0.55- and 10.5-μm attenuations within about 10% of each other.

Figure 5 shows the relation of visible and 1250-μm attenuation. These data contain even more scatter than the data in Figure 4. The correlation coefficient for the two attenuations is only 0.49. The correlation between 0.55-μm attenuation and 870-μm attenuation is 0.58.

Figure 6 shows that 10.5-μm attenuation is more closely related to 1250-μm attenuation in fog than it is to 0.55-μm attenuation. The correlation between these two sets of data is 0.9664.

The correlation between 10.5-μm attenuation and 870-μm attenuation is 0.9668 for the 65 fog drop-size distributions used in this study.

Figure 7 contains a plot of 870-μm attenuation versus 1250-μm attenuation. It is obvious that these data are very closely correlated. The correlation coefficient is 0.9873.

Platt (1970) made various approximations and computed an attenuation by fog at 1000 μm of 15.2 dB/km per g/m^3.

V. SUMMARY AND CONCLUSIONS

Extinction of electromagnetic energy by fog droplets depends upon the wavelength of the energy, the complex index of refraction of the drops for that wavelength, and the drop-size distribution.

No clear air attenuation is considered in this report. Webster (1973) has provided a good model of atmospheric molecular attenuation. Water vapor will be considered in a future report.

This report considers the following four wavelengths: 0.55 μm in the visible; 10.5 μm in the infrared; 870 μm in the submillimeter range; and 1250 μm. Measurements of the complex indices of refraction at these wavelengths for water do not vary much more than about 10% in any study. Variations are much less for the shorter wavelengths. Furthermore, the results of the computations are not influenced much by small changes in the complex index of refraction.

An extensive literature survey shows that the radius of fog droplets can vary from less than 1 μm to more than 100 μm. However, a large portion of drops have radii less than 20 μm, and few radii are greater than 40 μm. In some fogs the maximum radius is as small as 7.5 μm, but in other fogs more than half the drops have radii greater than 8 μm. These large variations sometimes occur in one location. There may also be large spatial and temporal variations within a fog.

Extinction of energy with a wavelength of 1250 μm is less than extinction of energy with a wavelength of 870 μm, regardless of the fog drop-size distribution.

The extinction of these wavelengths near 1 mm by fog droplets is less than the extinction of 0.55 and 10.5 μm in all fogs.

The way the extinction coefficient of 10.5-μm energy compares to the extinction coefficient of 0.55-μm energy depends upon the drop-size distribution. If the maximum drop radius is less than 10 μm, extinction of a wavelength of 10.5 μm is less than extinction of a wavelength of 0.55 μm. If most of the drop radii are greater than 10 μm, the extinction of energy with a wavelength of 10.5 μm is greater than the extinction of energy with a wavelength of 0.55 μm. Even a concentration of a fraction of a drop per cubic centimeter with a radius near 30 μm is important because the contribution of a drop to the extinction coefficient depends upon the square of the radius. Computations based upon fog drop-size distributions found in the literature indicate that extinction of the 10.5-μm wavelength is about the same as the extinction of the 0.55-μm wavelength in many fogs.

REFERENCES

Anyz, F., 1964: "Measurement of Water Content of Fogs in Industrial Regions," (in Russian). Studia Geophysica et Geodaetica, 8, 395-404.

Apletalin, V. N., V. V. Meriakri, and Y. Y. Chigryay, 1970: "Measurement of the Absorbing and Reflecting Properties of Water at Wavelengths from 2 to 0.8 mm," Radio Eng. Elect. Phys., 15, 1286-1288.

Arnulf, A., J. Bricard, E. Curé, and C. Véret, 1957: "Transmission by Haze and Fog in the Spectral Region 0.35 to 10 microns," J. Opt. Soc. Amer., 47, 491-498.

Baronti, P. and S. Elzweig, 1973: "A Study of Droplet Spectra in Fogs," J. Atmos. Sci., 30, 903-908.

Barteneva, O. D. and E. A. Polyakova, 1965: "A Study of Attenuation and Scattering of Light in a Natural Fog Due to its Microphysical Properties," Atmos. Oceanic Phys., 1, 114-121.

Berry, F. A., E. Bollay, and N. R. Beers (Editors), 1945: Handbook of Meteorology, McGraw-Hill Book Co., Inc., New York, pp. 727-736.

Best, A. C., 1951: "Drop-Size Distribution in Cloud and Fog," Quart. J. Roy. Meteor. Soc., 77, 418-426.

Bisyarin, V. P., I. P. Bisyarina, and A. V. Sokolov, 1971: "Attenuation of 10.6 μm Laser Radiation in Artificial and Real Fog," Radio Eng. Elect. Phys., 16, 1589-1594.

Carlon, H. R., 1970: "Infrared Emission by Fine Water Aerosols and Fogs," Appl. Optics, 9, 2000-2006.

Chamberlain, J., M. S. Zafar, and J. B. Hasted, 1973: "Direct Measurement of Refraction Spectrum of Liquid Water at Submillimetre Wavelengths," Nature, Phys. Sci., 243, 116-117.

Chisholm, D. A. and H. Kruse, 1974: The Variability of Visibility in the Hanscom Mesonetwork: A Preliminary Assessment. Air Force Cambridge Research Laboratories Report AFCRL-TR-74-0265, Environmental Research Paper AFCRL-ERP-479, NTIS Catalog No. AD-784791, 32 pp.

Chu, T. S. and D. C. Hogg, 1968: "Effects of Precipitation on Propagation at 0.63, 3.5, and 10.6 microns," The Bell System Tech. J., 47, 723-759.

Chýlek, P., 1975: "Asymptotic Limits of the Mie-Scattering Characteristics," J. Opt. Soc. Amer., 65, 1316-1318.

Chýlek, P., 1977: "A Note on Extinction and Scattering Efficiencies," J. Appl. Meteor., 16, 321-322.

Cong, L. P. and J. Dessens, 1973: "Brouillards Artificiels Produits par Émission Industrielle de Vapeur d'Eau" J. Rech. Atmos., 7, 109-116.

Davies, M., G. W. F. Pardoe, J. Chamberlain, and H. A. Gebbie, 1970: "Submillimetre- and Millimetre-Wave Absorptions of Some Polar and Non-polar Liquids Measured by Fourier Transform Spectorscopy," Trans. Faraday Soc., 66, Part 2, 273-292.

Deirmendjian, D., 1975: "Far-Infrared and Submillimeter Wave Attenuation by Clouds and Rain," J. Appl. Meteor., 14, 1584-1593.

Deirmendjian, D., R. Clasen, and W. Viezee, 1961: "Mie Scattering with Complex Index of Refraction," J. Opt. Soc. Amer., 51, 620-633.

Deloncle, M., 1963a: "Constitution des Brouillards Urbains," J. Rech. Atmos., 1, 107-111.

Deloncle, M., 1963b: "Étude Photoélectrique des Aérosols Volatils," Revue d'Optique Théorique et Instrumentale, 42, 157-196.

Dickson, D. R. and J. V. Hales, 1963: "Computation of Visual Range in Fog and Low Clouds," J. Appl. Meteor., 2, 281-285.

Dickson, D. H., R. B. Loveland, and W. H. Hatch, 1975: Atmospheric Waterdrop Size Distribution at Capistrano Test Site (CTS) from 16 April through 11 May 1974, Volumes I, II, III, IV, V, and VI. Report ECOM-DR 75-3.

Dobbins, R. A. and T. I. Eklund, 1977: "Ripple Structure of the Extinction Coefficient," Appl. Optics, 16, 281-282.

Donaldson, R. J., 1955: "Drop-Size Distribution, Liquid Water Content, Optical Transmission, and Radar Reflectivity in Fog and Drizzle." Proc. Fifth Wea. Radar Conf., 12-15 September 1955, Asbury Park, New Jersey, 275-280.

Donati, S., 1973: "Thermal Imaging Through Hazes and Fogs in the Middle and Far Infrared Windows: Some Experimental Results," Alta Frequenza (English Edition), 42, 101-104.

Downing, H. D. and D. Williams, 1975: "Optical Constants of Water in the Infrared," J. Geophys. Res., 80, 1656-1661.

Eldridge, R. G., 1961: "A Few Fog Drop-Size Distributions," J. Meteor., 18, 671-676.

Eldridge, R. G., 1966: "Haze and Fog Aerosol Distributions," J. Atmos. Sci., 23, 605-613.

Eldridge, R. G., 1969: "Mist — the Transition from Haze to Fog," Bull. Amer. Meteor. Soc., 50, 422-426.

Eldridge, R. G., 1971: "The Relationship Between Visibility and Liquid Water Content in Fog," J. Atmos. Sci., 28, 1183-1186.

Essenwanger, O. M., 1976: Comments on "Empirical Fog Droplet Size Distribution Functions with Finite Limits," J. Atmos. Sci., 33, 338-339.

Findeisen, W., 1932: "Messungen der Grösse und Anzahl der Nebeltropfen zum Studium der Koagulation Inhomogenen Nebels," Gerlands Beitraege zur Geophysik, 35, 295-340.

Flanigan, D. F. and H. P. DeLong, 1970: Spectral Absorption Characteristics of the Major Components of Dust Clouds. Edgewood Arsenal Technical Report EATR 4430, 57 pp.

Garland, J. A., 1971: "Some Fog Droplet Size Distributions Obtained by an Impaction Method," Quart. J. Roy. Meteor. Soc., 97, 483-494.

Garland, J. A., J. R. Branson, and L. C. Cox, 1973: "A Study of the Contribution of Pollution to Visibility in a Radiation Fog," Atmos. Environment, 7, 1079-1092.

Gathman, S. G. and R. E. Larson, 1974: Marine Fog Observations in the Arctic. Naval Research Laboratory Report 7693, NTIS Catalog Number AD-778999, 27 pp.

George, D. H., 1972: "Estimates of Fog Element Length," J. Appl. Meteor., 11, 874-876.

Gorchakov, G. I., A. A. Isakov, and L. N. Markina, 1972: "Determination of the Basic Parameters of Fog Microstructure from the Coronal Indicatrix," Atmos. Oceanic Phys., 8, 50-53.

Gordin, M. P. and G. M. Strelkov, 1975: "The Passage of Laser Radiation Through a Fine-Droplet Water Aerosol," Radio Eng. Elect. Phys., 20, No. 10, English, pp. 1-7.

Goronina, K. A., R. K. Belov, and E. P. Sorokina, 1966: "Dielectric Constant Measurement Based on the Variation of the Polarization of Reflected Waves," Sov. Radiophys., 9, 567-569.

Grunow, J., 1960: "The Productiveness of Fog Precipitation in Relation to the Cloud Droplet Spectrum," Physics of Precipitation, Geophysical Monograph Number 5, American Geophysical Union, pp. 110-117.

Gumprecht, R. O. and C. M. Sliepcevich, 1951: Tables of Light-Scattering Functions for Spherical Particles. Engineering Research Institute, Special Publications: Tables, University of Michigan, 593 pp.

Hagemann, V., 1936: "Eine Methode zur Bestimmung der Grösse der Nebel- und Wolkenelemente," Gerlands Beitraege zur Geophysik, 46, 261-282.

Hale, G. M. and M. R. Querry, 1973: "Optical Constants of Water in the 200-nm to 200-μm Wavelength Region," Appl. Optics., 12, 555-563.

Hänel, G., 1971: "New Results Concerning the Dependence of Visibility on Relative Humidity and Their Significance in a Model for Visibility Forecast," Beitr. Phys. Atmos., 44, 137-167.

Hoidale, G. B. and A. J. Blanco, 1969: "Infrared Absorption Spectra of Atmospheric Dust Over an Interior Desert Basin," Pure Appl. Geophys., 74, 151-164.

Houghton, H. G. and W. H. Radford, 1938: "On the Measurement of Drop Size and Liquid Water Content in Fogs and Clouds," Papers Phys. Oceanogr. Meteor., 6, No. 4, 31 pp.

Huschke, R. E. (Editor), 1959: Glossary of Meteorology. American Meteorological Society, Boston, Massachusetts, 645 pp.

Irvine, W. M. and J. B. Pollack, 1968: "Infrared Optical Properties of Water and Ice Spheres," Icarus, 8, 324-360.

Jiusto, J. E., 1964: Investigation of Warm Fog Properties and Fog Modification Concepts. NASA Contract Report CR-72, Contract NASr-156, Cornell Aeronautical Laboratory, Buffalo, New York.

Jiusto, J. E., 1974: "Remarks on Visibility in Fog," J. Appl. Meteor., 13, 608-610.

Johnson, J. C., 1954: Physical Meteorology. Published jointly by the Technology Press of the Massachusetts Institute of Technology and John Wiley and Sons, Inc., New York, 403 pp.

Johnson, D. B , 1976: "Ultragiant Urban Aerosol Particles," Science, 194, 941-942.

Johnston, D. R. and D. E. Burch, 1967: "Attenuation by Artificial Fogs in the Visible, Near Infrared, and Far Infrared," Appl. Optics, 6, 1497-1501.

Kerker, M., 1969: The Scattering of Light and Other Electromagnetic Radiation. Academic Press, New York, pp. 27-75.

Kislovskii, L. D., 1959: "Optical Characteristics of Water and Ice in the Infrared and Radiowave Regions of the Spectrum," Optics and Spectroscopy, 7, 201-206.

Koester, K. L and L. H. Kosowsky, 1970: "Attenuation of Millimeter Waves in Fog," Fourteenth Radar Meteorology Conference, Preprints, 231-236.

Kozima, K., T. Ono, and K. Yamaji, 1953: "The Size Distribution of Fog Particles," Studies on Fogs, Hokkaido University, 303-309.

Kumai, M., 1973: "Arctic Fog Droplet Size Distribution and its Effect on Light Attenuation," J. Atmos. Sci., 30, 635-643.

Kunkel, B. A., 1971: "Fog Drop-Size Distributions Measured with a Laser Hologram Camera," J. Appl. Meteor., 10, 482-486.

Laktionov, A. G., 1967a: "On the Connection Between the Condensation Activity of Irradiated Nuclei and Their Sizes," Atmos. Oceanic Phys., 3, 13-17.

Laktionov, A. G., 1967b: "Variation of the Size and Concentration of Drops During the Scattering of Fog," Atmos. Oceanic Phys., 3, 321-323.

Laktionov, A. G., Yu. S. Lyubovtseva, and M. S. Malkevich, 1973: "Certain Statistical Characteristics of Aerosol Microstructure in the Surface Layer of the Atmosphere," Atmos. Oceanic Phys., 9, 73-76.

Lala, G. G., E. Mandel, and J. E. Jiusto, 1975: "A Numerical Evaluation of Radiation Fog Variables," J. Atmos. Sci., 32, 720-728.

Landsberg, H., 1958: Physical Climatology. Gray Printing Co., DuBois, Pennsylvania, pp. 138-141.

Low, R. D. H., 1975a: "Microphysical Evolution of Fog." J. Rech. Atmos., 9, 23-32.

Low, R. D. H., 1975b: "Microphysical and Meteorological Measurements of Fog Supersaturation," Tellus, 27, 507-513.

Ludwig, F. L., S. Schechter, R. C. Robbins, and J. H. Smith, 1974: Condensation Nuclei and Aerosol Populations Related to Fog Formation. Final Report II, SRI Project 6676, prepared under Army Contract DAHC04-67-C-0059, completed December 1973 and printed January 1974, 212 pp.

McCartney, E. J., 1976: Optics of the Atmosphere, John Wiley and Sons, New York, 408 pp.

Mack, E. J., R J Pilié, W. C. Kocmond, 1973: An Investigation of the Microphysical and Micrometeorological Properties of Sea Fog. Calspan No. CJ-5237-M-1, 40 pp.

Magono, C., T. Harimaya, and S. Adachi, 1974: "An Observation of the Modification of a Mesoscale Cold Air Mass Over a Warm Sea Surface, Utilizing the Height and Temperature of Steam Fog Top," J. Meteor. Soc. Japan, 52, 491-497.

Mallow, J. V., 1975: "Empirical Fog Droplet Size Distribution Functions with Finite Limits," J. Atmos. Sci., 32, 440-443.

May, K. R., 1961: "Fog-Droplet Sampling Using a Modified Impactor Technique," Quart. J. Roy. Meteor. Soc., 87, 535-548.

Mészaros, A., 1965: "Concentration et Distribution Dimensionnelle des Gouttelettes de Brouillards Atmosphériques," J. Rech. Atmos., 2, 53-64.

Mészaros, A., 1971: "On the Variation of the Size Distribution of Large and Giant Atmospheric Particles as a function of the Relative Humidity," Tellus, 23, 436-440.

Mie, G., 1908: "Beiträge zur Optik Trüber Medien, Speziell Kolloidaler Metallösungen," Annalen der Physik, 25, fourth series, 377-445.

Okita, T., 1962: "Observations of the Vertical Structure of a Stratus Cloud and Radiation Fogs in Relation to the Mechanism of Drizzle Formation," Tellus, 14, 310-322.

Pedersen, K. and M. Todsen, 1960: "Some Measurements of the Microstructure of Fog and Stratus Clouds in the Oslo-Area," Geofysiske Publikasjoner, 21, No. 7, 1-16.

Penndorf, R., 1957: "New Tables of Total Mie Scattering Coefficients for Spherical Particles of Real Refractive Index," J. Opt. Soc. Amer., 47, 1010-1015.

Pilié, R. J., E. J. Mack, W. C. Kocmond, C. W. Rogers, and W. J. Eadie, 1975a: "The Life Cycle of Valley Fog, Part I: Micrometeorological Characteristics," J. Appl. Meteor., 14, 347-363.

Pilié, R. J., E. J. Mack, W. C. Kocmond, W. J. Eadie, and C. W. Rogers, 1975b: "The Life Cycle of Valley Fog, Part II: Fog Microphysics," J. Appl. Meteor., 14, 364-374.

Platt, C. M. R., 1970: "Transmission of Submillimeter Waves Through Water Clouds and Fogs," J. Atmos. Sci., 27, 421-425.

Querry, M. R., W. E. Holland, R. C. Waring, L. M. Earls, and M. D. Querry, 1977: "Relative Reflectance and Complex Refractive Index in the Infrared for Saline Environmental Waters," J. Geophys. Res., 82, 1425-1433.

Reinking, R. F., 1975: Project Foggy Cloud VII — Warm Fog Dispersal and Prevention (Preliminary Summary). Naval Weapons Center Technical Memorandum 2527, 30 pp.

Rensch, D. B. and R. K. Long, 1970: "Comparative Studies of Extinction and Backscattering by Aerosols, Fog, and Rain at 10.6 μ and 0.63 μ," Appl. Optics, 9, 1563-1573.

Richer, K. A., 1970: "Environmental Effects on Radar and Radiometric Systems at Millimeter Wavelengths," Proc. Symposium on Submillimeter Waves, Polytechnic Institute of Brooklyn, 31 March — 2 April 1970, pp. 533-543.

Roberts, R. E., 1976: Atmospheric Transmission Modeling: Proposed Aerosol Methodology with Application to the Grafenwöhr Atmospheric Optics Data Base. Institute for Defense Analysis Paper P-1225, 24 pp.

Rodhe, B., 1962: "The Effect of Turbulence on Fog Formation," Tellus, 14, 49-86.

Rodhe, B., 1966: "The Concentration of Liquid Water in the Atmosphere," Tellus, 18, 86-104.

Rogers, C. W., E. J. Mack, U. Katz, C. C. Easterbrook, and R. J. Pilié, 1974: The Life Cycle of California Coastal Fog Onshore. Calspan Report No. CJ-5076-M-3 for Air Force Cambridge Research Laboratories, Cambridge, Massachusetts, AFCRL-TR-74-0419, 85 pp.

Rozenberg, V. I., 1974: Scattering and Attenuation of Electromagnetic Radiation by Atmospheric Particles. NASA Technical Translation F-771 of a Russian Hydrometeorological Press Publication in Leningrad in 1972, 339 pp.

Schönwiese, V. C. D., 1970: "Zur Systematik der Nebelerscheinungen," Wetter and Leben, 22, 185-190.

Stalenhoef, A. H. C., 1974: "Slant Visibility During Fog Related to Wind Speed, Air Temperature and Stability," Arch. Meteor. Geophys. Bioklim., Ser. B., 22, 351-361.

Stephens, J. J., P. S. Ray, and R. J. Kurzeja, 1971: "Far-Field Transient Backscattering by Water Drops," J. Atmos. Sci., 28, 785-793.

Tag, P. M., 1976: "A Numerical Simulation of Warm Fog Dissipation by Electrically Enhanced Coalescence: Part I. An Applied Electric Field," J. Appl. Meteor., 15, 282-291.

Tampieri, F. and C. Tomasi, 1976a: "Size Distribution Models of Fog and Cloud Droplets in Terms of the Modified Gamma Function," Tellus, 28, 333-347.

Tampieri, F. and C. Tomasi, 1976b: "Size Distribution Models of Fog and Cloud Droplets and Their Volume Extinction Coefficients at Visible and Infrared Wavelengths," Pure and Appl. Geophys., 114, 571-586.

Thompson, B. J., J. H. Ward, and W. R. Zinky, 1967: "Application of Hologram Techniques for Particle Size Analysis," Appl. Optics, 6, 519-526.

Thuman, W. C. and E. Robinson, 1954: "Studies of Alaskan Ice-Fog Particles," J. Meteor., 11, 151-156.

Tverskoi, P. N., 1965: Physics of the Atmosphere. Translated from Russian for the National Aeronautics and Space Administration and the National Science Foundation, NASA TTF-288 TT65-50114, 314-343.

US National Bureau of Standards Computation Laboratory, 1949: Tables of Scattering Functions for Spherical Particles. Applied Mathematics Series, 4. Washington, D.C., US Government Printing Office, Printed 1948, issued January 1949, 120 pp.

Verner, B., 1976: "Note on the Recurrence Between Mie's Coefficients," J. Opt. Soc. Amer., 66, 1424-1425.

Webb, W. L., 1956: "Particulate Counts in Natural Clouds and Fogs," J. Meteor., 13, 203-206.

Webster, D. W., 1973: Military Potential of the Extreme Infrared: Technology and Applications. Naval Weapons Center Report TP 5565. Catalogued under AD915347.

Weeks, W. L., 1964: Electromagnetic Theory for Engineering Applications. John Wiley and Sons, New York, 744 pp.

Weinstein, A. I., 1974a: Air Pollution and Warm Fog Modification, Air Force Cambridge Research Laboratories Report AFCRL-TR-74-0289, Cambridge, Massachusetts. Environmental Research Paper AFCRL-ERP-480, NTIS Catalog No. AD-786454, 16 pp.

Weinstein, A. I., 1974b: "Air Pollution and Warm Fog Dispersal," Proc. Conf. on Wea. Modification, Amer. Meteor. Soc., 18-21 November 1974, pp. 282-285.

Wells, W. C., G. Gal, and M. W. Munn, 1977: "Aerosol Distributions in Maritime Air and Predicted Scattering Coefficients in the Infrared," Appl. Optics, 16, 654-659.

Zerull, R. H., R. H. Giese, and K. Weiss, 1977: "Scattering Functions of Nonspherical Dielectric and Absorbing Particles vs Mie Theory," Appl. Optics, 16, 777-778.

Zuev, V. E., I. V. Samokhvalov, and Yu. S. Balin, 1972: "Investigation of the Ground Layer of the Atmosphere and Clouds Using Laser Location," Sov. Phys. J., 15, 730-732.

DISTRIBUTION

	No. of Copies
US Army Missile R&D Command Basic Distribution List	34
Defense Documentation Center Cameron Station Alexandria, Virginia 22314	12
Colorado State University Department of Atmospheric Science ATTN: Prof. E. Reiter Fort Collins, Colorado 80523	1
Office of Naval Research/Code 221 ATTN: D. C. Lewis 800 N Quincy Street Arlington, Virginia 22217	1
Pacific Missile Test Center Code 3253 ATTN: Charles Phillips Point Mugu, California 93042	1
Commander US Continental Army Command ATTN: Reconnaissance Branch ODSC for Intelligence Fort Monroe, Virginia 23351	1
Commander US Army Test and Evaluation Command ATTN: NBC Directorate AMSTE-EL -BAF Aberdeen Proving Ground, Maryland 21005	1 1 1
Commander US Army Cold Regions Research and Engineering Laboratories ATTN: Environmental Research Branch Hannover, New Hampshire 03755	1
Commander US Army Ballistics Research Laboratories ATTN: AMXBR-B -LA ATTN: Ken Richer Aberdeen Proving Ground, Maryland 21005	1 1 1
Commander US Army Edgewood Arsenal ATTN: SMUEA-CS-O Operations Research Group Edgewood Arsenal, Maryland 21010	1
Commander US Army Frankford Arsenal ATTN: SMUFA-1140 Philadelphia, Pennsylvania 19137	1
Commander US Army Picatinny Arsenal ATTN: SMUPS-TV-3 Dover, New Jersey 07801	1

	No. of Copies
Optical Science Consultants ATTN: Dr. D. L. Fried P. O. Box 388 Yorba Linda, California 92686	1
ADTC/XRCE ATTN: D. Dingus Eglin Air Force Base, Florida 32542	1
Commander AFATL/LMT Eglin Air Force Base, Florida 32544	1
Commander US Army Dugway Proving Ground ATTN: Meteorology Division Dugway, Utah 84022	1
Commander US Army Artillery Combat Developments Agency Fort Sill, Oklahoma 73504	1
Commander US Army Artillery and Missile School ATTN: Target Acquisition Department Fort Sill, Oklahoma 73504	1
Commander US Army Communications — Electronics Combat Development Agency Fort Huachuca, Arizona 85613	1
Commander Desert Test Center Fort Douglas, Utah 84113	1
Commander US Army CBR School Micrometeorological Section Fort McClellan, Alabama 36205	1
Commander USAF Air Weather Service (MATS) ATTN: AWS/DNTI Scott Air Force Base, Illinois 62225	1
Commander US Army Combined Arms Combat Development Activity Fort Leavenworth, Kansas 66027	1
Chief of Naval Operations ATTN: Code 427 Department of the Navy Washington, D.C. 20350	1
Chief US Weather Bureau ATTN: Librarian Washington, D.C. 20235	1

	No. of Copies
Control Data Corporation Research Division ATTN: Dr. Belmont Minneapolis, Minnesota 55440	1
Georgia Institute of Technology Engineering Experiment Station ATTN: James Gallager 347 Ferst Drive Atlanta, Georgia 30332	1
Director US Army Engineer Waterways Experiment Station ATTN: WESSR Vicksburg, Mississippi 39101	1
Director Atmospheric Sciences Program National Sciences Foundation Washington, D.C. 20550	1
Director Bureau of Research and Development Federal Aviation Agency Washington, D.C. 20553	
Commander US Army Aviation Systems Command 12th and Spruce Streets St. Louis, Missouri 63166	1
Director US Army Air Mobility Research and Development Laboratory Ames Research Center Moffett Field, California 94035	1
Director of Meteorological Systems Office of Applications (FM) National Aeronautics and Space Administration Washington, D.C. 20546	1
Environmental Research Institute of Michigan Infrared and Optics Division ATTN: Anthony J. LaRocca Robert L. Spellicy P. O. Box 618 Ann Arbor, Michigan 48107	1 1
Kaman Nuclear ATTN: Lora Guy, Assistant Librarian Garden of the Gods Road Colorado Springs, Colorado 80907	1
Lockheed Missile and Space Company Department 81 - 73 ATTN: Mr. H. R. Allison Sunnyvale, California 94088	1
Lockheed-California Company Department 72 - 25 ATTN: Dr. L. Baer Burbank, California 91503	1
Massachusetts Institute of Technology ATTN: Department of Meteorology Cambridge, Massachusetts 02139	1
Meteorological and Geoastrophysical Abstract Editorial Office P. O. Box 1736 Washington, D.C. 20013	
The Rand Corporation ATTN: Dr. S. J. Dudzinsky, Jr. 1700 Main Street Santa Monica, California 90406	2
Commander Center for Naval Analyses ATTN: Document Control 1401 Wilson Boulevard Arlington, Virginia 22209	1
Martin Company ATTN: Engineering Library Mail J1-398 Baltimore, Maryland 21203	1
National Bureau of Standards Boulder Laboratories ATTN: Library Boulder, Colorado 80302	1
Navy Representative National Climatic Center Arcade Building Asheville, North Carolina 28801	1
National Oceanic and Atmospheric Administration National Climatic Center ATTN: Technical Library Arcade Building Asheville, North Carolina 28801	1
Director Defense Advanced Research Projects Agency 1400 Wilson Boulevard Arlington, Virginia 22209	1
Honeywell, Inc. Systems and Research Division ATTN: Dr. Paul Kruse Minneapolis, Minnesota 55413	1

No. of Copies

Raytheon Company
ATTN: A. V. Jelalian 1
528 Boston Post Road
Sudbury, Massachusetts 01776

National Aeonautics and Space Administration
Marshall Space Flight Center
ATTN: R-AERO-Y 1
Marshall Space Flight Center, Alabama 35812

National Center for Atmospheric Research
ATTN: Library 1
Boulder, Colorado 80302

Director of Defense Research and Engineering
Engineering Technology
ATTN: Mr. L. Weisberg 2
Washington, D.C. 20301

Office of Chief Communications-Electronics
Department of the Army
ATTN: Electronics Systems Directorate 1
Washington, D.C. 20315

Office, Assistant Chief of Staff for Intelligence
Department of the Army
ATTN: ACSI-DSRSI 1
Washington, D.C 20310

Office of US Naval Weather Service
US Naval Air Station
Washington, D.C. 20390 1

Office, Assistant Secretary of Defense
Research and Engineering
ATTN: Technical Library 1
Washington, D.C. 20301

Pennsylvania State University
ATTN: Department of Meteorology 1
University Park, Pennsylvania 16802

Commander
US Air Force Avionics Laboratory
ATTN: D. Rees 1
CPT James D. Pryce, AFAL/WE 1
Dr. B. L. Sowers, AFAL/RWI 1
Wright Patterson Air Force Base, Ohio 45433

University of Washington
ATTN: Department of Meteorology 1
Seattle, Washington 98105

University of Chicago
Department of Meteorology
Chicago, Illinois 60637 1

No. of Copies

University of Wisconsin
ATTN: Prof. Weinman 1
Prof. E. Wahl 1
Madison, Wisconsin 53706

US Army Engineering Topographic Laboratories
Earth Sciences Division
ATTN: ETL-GS-ES, Dr. William B. Brierly 1
Fort Belvoir, Virginia 22060

Commander
US Army Research Office
ATTN: Dr. R. Lontz 2
P. O. Box 12211
North Carolina 27709

US Army Research and Standardization Group (Europe)
ATTN: DRXSN-E-RX
Dr. Alfred K. Nedoluha 2
Box 65
FPO New York 90510

US Army Materiel Development and Readiness Command
ATTN: Dr. Gordon Bushy 1
Dr. James Bender 1
Dr. Edward Sedlak 1
5001 Eisenhower Avenue
Alexandria, Virginia 22333

Commander
US Army Tank Automotive Development Command
ATTN: DRDTA-RWL 1
Warren, Michigan 48090

Commander
US Army Mobility Equipment Research and Development Command
Fort Belvoir, Virginia 22060

Commander
US Army Harry Diamond Laboratories
2800 Powder Mill Road
ATTN: Dr. Stan Kulpa 1
Adelphi, Maryland 20783

Commander
US Army Armament Command
Rock Island, Illinois 61202 1

Commander
US Army Foreign Science and Technology Center
Federal Office Building
220 7th Street, NE
Charlottesville, Virginia 22901 1

	No. of Copies
Commander	
US Army Training and Doctrine Command	
Fort Monroe, Virginia 23351	1
Director	
Ballistic Missile Defense Advanced Technology Center	
ATTN: ATC-D	1
ATC-O	1
ATC-R	1
ATC-T	1
P. O. Box 1500	
Huntsville, Alabama 35807	
Commander	
US Naval Air Systems Command	
Washington, D.C. 20360	1
Chief of Naval Research Department of the Navy	
Washington, D.C. 20360	1
Commander	
US Naval Air Development Center	
Warminster, Pennsylvania 18974	1
Commander	
US Naval Electronics Lab Center	
San Diego, California 92152	1
Commander	
US Naval Surface Weapons Center	
Dahlgren, Virginia 22448	1
ElectroScience Laboratory	
Department of Electrical Engineering	
The Ohio State University	
ATTN: Dr. Ronald K. Long	1
1320 Kinnear Road	
Columbus, Ohio 43212	
Commander	
US Air Force, AFOSR/NP	
ATTN: LT COL Gordon Wepfer	1
Bolling Air Force Base	
Washington, D.C. 20332	
Naval Surface Weapons Center	
ATTN: Mary Tobin	1
WR42	
White Oak, Maryland 20910	
Pacific-Sierra Research Corporation	
Alan R. Shapiro	1
Vice President	
1456 Cloverfield Boulevard	
Santa Monica, California 90404	
The Aerospace Corporation	
ATTN: Dr. D. T. Hodges, Jr.	1
C. M. Randall	1
Box 92957	
2350 East El Segundo Boulevard	
Los Angeles, California 90009	
Headquarters	
Department of the Army	
ATTN: DAEN-RDM/Dr. F. de Percin	1
Washington, D.C. 20314	
Commander	
USAF Environmental Technical Applications Center (MAC)	
ATTN: Mr. Oscar E. Richard	1
Box 825	
Scott Air Force Base, Illinois 62225	
Headquarters	
Department of the Army	
Directorate of Army Research	
ATTN: DAMA-ARZ	2
DAMA-ARZ-D/	
Dr. Frank D. Verderame	1
Washington, D.C. 20310	
Dr. Robert J. Renard	1
Department of Meteorology	
Naval Postgraduate School	
Monterey, California 93940	
Dr. John J. DeLuisi	1
NOAA/ERL-ARL	
Boulder, Colorado 80303	
Director	
US Army Night Vision Laboratory	
ATTN: Mr. John Johnson	1
Mr. Joseph R. Moulton	1
Fort Belvoir, Virginia 22060	1
Science and Technology Division	
Institute for Defense Analyses	
ATTN: Dr. Vincent J. Corcoran	1
Dr. Robert E. Roberts	1
Dr. Lucien M. Biberman	1
400 Army-Navy Drive	
Arlington, Virginia 22202	
Director	
Naval Research Laboratory	
ATTN: Code 5300, Radar Division	1
Code 5370, Radar Geophysics Branch	1
Code 5460, Electromagnetic Propagation Branch	1
Washington, D.C. 20390	
Florida State University	
ATTN: Prof. Dr. Gleeson	1
Prof. Dr. Craig	1
Dept. of Meteorology Library	1
Tallahassee, Florida 32306	

	No. of Copies
Air Force Cambridge Research Laboratories	
ATTN: OPI, Mr. John Selby	1
CRXL	1
LKI, Mr. Lund	1
Mr. Gringorten	1
Mr. Lenhard	1
Mr. Grantham	1
LYS, Mr. R. S. Hawkins	1
Mr. V. Falcone	1
LYW, Mrs. R. M. Dyer	1
Mr. R. J. Donaldson	1
LYP, Mr. B. A. Kunkel	1
L. G. Hanscom Field	
Bedford, Massachusetts 01731	
Commander	
US Army Electronics Command	
ATTN: DRSEL-RD-SM, Mr. M. Lowenthal	1
-TL-1, Dr. Jacobs	1
-CT, Dr. R. Buser	1
Fort Monmouth, New Jersey 07703	
Commander	
Naval Weapons Center	
ATTN: Code 3173, Dr. Alexis Shlanta	1
Mr. Robert Moore	1
China Lake, California 93555	
Commander/ Director	
Atmospheric Sciences Laboratory	
US Army Electronics Command	
ATTN: DRSEL-BL-DD, Mr. Rachele	3
Dr. Mishri Vatsia	1
Mr. James D. Lindberg	1
White Sands Missile Range, New New Mexico 88002	
Superior Technical Services, Inc.	
ATTN: D. Creel	1
4308 Governors Drive	
Huntsville, Alabama 35802	
DRSMI-LP, Mr. Voigt	1
DRCPM-LD	1
-LD, COL J. H. Reeves	1
DRDMI-X, Dr. McDaniel	1
-XS, Dr. Hallowes	1
-T, Dr. Kobler	1
-H, Dr. Rose	1
-TD, Dr. McCorkle	1
Mr. Sullivan	1
Mr. Conrad	1
-TE, Mr. Lindberg	1
Mr. Pittman	1
-TG, Mr. Huff	1
-TK	1

	No. of Copies
DRDMI-TKP, Mr. Duerr	1
-TL, Mr. Lewis	1
-TLD, Mr. Truman Gregg	1
-E, Mr. Northrop	1
-C	1
-CE, Mr. S. L. Johnston	1
-TB, Mr. Clark	1
-TBL	5
-TP, Mr. Bledsoe	1
-TPR	1
-TR, Dr. Hartman	1
Dr. Bennett	1
Mrs. Davis	3
-TRA, Dr. Essenwanger	1
Dr. Gibson	1
Mr. Dudel	1
Dr. Lilly	1
Dr. Stewart	50
Mrs. Boyd	1
-TRD, Mr. Shatas	1
-TRO, Dr. Stettler	1
Dr. Guenther	1
Dr. Gamble	1
Mr. Osmundsen	1
-TBD	3
-TI (Record Set)	1
(Reference Copy)	1